


Fall 12-14-2018

Computational Spectroscopy of C-Like Mg VII

Saleh Allehabi
saleh.allehabi@students.cau.edu

Follow this and additional works at: <http://digitalcommons.auctr.edu/cauetds>

 Part of the [Atomic, Molecular and Optical Physics Commons](#), and the [Quantum Physics Commons](#)

Recommended Citation

Allehabi, Saleh, "Computational Spectroscopy of C-Like Mg VII" (2018). *Electronic Theses & Dissertations Collection for Atlanta University & Clark Atlanta University*. 153.
<http://digitalcommons.auctr.edu/cauetds/153>

This Thesis is brought to you for free and open access by the Clark Atlanta University at DigitalCommons@Robert W. Woodruff Library, Atlanta University Center. It has been accepted for inclusion in Electronic Theses & Dissertations Collection for Atlanta University & Clark Atlanta University by an authorized administrator of DigitalCommons@Robert W. Woodruff Library, Atlanta University Center. For more information, please contact cwiseman@auctr.edu.

ABSTRACT

DEPARTMENT OF PHYSICS

ALLEHABI, SALEH

B.S. TAIBAH UNIVERSITY, 2007

COMPUTATIONAL SPECTROSCOPY OF C-LIKE Mg VII

Committee Chair: Swaraj S. Tayal, Ph.D.

Thesis dated December 2018

In this thesis, energy levels, lifetimes, oscillator strengths and transition probabilities of Mg VII have been calculated. The Hartree-Fock (HF) and Multiconfiguration Hartree-Fock (MCHF) methods were used in the calculations of these atomic properties. We have included relativistic operators mass correction, spin-orbit interaction, one body Darwin term and spin-other-orbit interaction in the Breit-Pauli Hamiltonian. The configurations, $(1s^2)2s^22p^2$, $2s2p^3$, $2p^4$, $2s^22p3s$, $2s^22p3p$, $2s2p^2(^4P)3s$ and $2s^22p3d$ which correspond to 52 fine-structure levels, were included in the atomic model for the Mg VII ions. The present results have been compared with NIST compilation and other theoretical results, and generally a good agreement was found.

COMPUTATIONAL SPECTROSCOPY OF C-LIKE Mg VII

A THESIS

SUBMITTED TO THE FACULTY OF CLARK ATLANTA UNIVERSITY

IN PARTIAL FULFILLMENT OF THE REQUIREMENTS FOR

THE DEGREE OF MASTER OF SCIENCE

BY

SALEH ALLEHABI

DEPARTMENT OF PHYSICS

ATLANTA, GEORGIA

DECEMBER 2018

© 2018

SALEH ALLEHABI

All Rights Reserved

ACKNOWLEDGMENTS

It is a pleasure to express my deep sense of thanks and gratitude to my advisor, Dr. Swaraj S. Tayal, for his dedication and keen interest in helping me complete my project. I thank him for his time and effort that he devoted to support me during this project.

I would like to give special thanks to all my graduate professors, especially Drs. Wang, Msezane, and Mickens for their encouragement and support. I owe a deep sense of gratitude to Drs. Msezane and Wang who were a part of my thesis committee. They offered guidance throughout my entire journey.

I also thank Ms. Heard for her encouragement and for everything she did to assist me. I would like to thank my classmate, Mohamed Kerwat, for his help and support. I am thankful to all other faculty and staff members in the department of physics for their kind cooperation and assistance.

I would like to acknowledge with gratitude, my parents for teaching me early in my childhood and I appreciate their continued encouragement and support. Finally, I thank my wife for her continuous support throughout the duration of my studies. She always stood by me and kept me going.

TABLE OF CONTENTS

ACKNOWLEDGMENTS	ii
LIST OF FIGURES	iv
LIST OF TABLES	v
LIST OF ABBREVIATIONS.....	vi
CHAPTER	
1. INTRODUCTION	1
2. COMPUTATIONAL METHODS.....	5
2.1 Non-relativistic Method	5
2.2 Semi-relativistic Method	10
3. RESULTS AND DISCUSSION	19
3.1 Energy Levels	19
3.2 Lifetimes.....	24
3.3 Oscillator Strengths and Transition Probabilities	27
3.3.1 Oscillator Strengths and Transition Probabilities for some E1 Transitions	27
3.3.2 Transition Probabilities for Forbidden E2 and M1 Transitions	40
4. CONCLUSION.....	44
REFERENCES	46

LIST OF FIGURES

Figure

1. Fine-structure and term splitting of the $1s^22s^22p^2$ configuration 16
2. Comparison between the present and Kelleher and Podobedova [9] calculated transition probabilities for some E1 transitions 32
3. Comparison between length and velocity forms of present oscillator strengths for some E1 transitions 38
4. Comparison of calculated length form of oscillator strengths for some E1 transitions with Froese Fischer and Tachiev [13] 39
5. Comparison of length and velocity forms of the present oscillator strengths as a function of length form of present values for some E1 transitions 40

LIST OF TABLES

Table

I. Comparison of present excited energy levels of Mg VII (Ry) with other calculations.....	20
II. Comparison of lifetimes (s) of Mg VII levels with other calculations.....	24
III. Comparison of oscillator strengths and transition probabilities (s^{-1}) for some E1 transitions with other calculations	28
IV. Comparison of length and velocity oscillator strengths for some E1 transitions with Froese Fischer and Tachiev [13]	33
V. Comparison of transition probabilities (s^{-1}) for forbidden E2 and M1 transitions with other calculations	41

LIST OF ABBREVIATIONS

Mg VII	Mg ⁶⁺ ions
HF	Hartree-Fock
MCHF	Multiconfiguration Hartree-Fock
SS	SUPERSTRUCTURE
GRASP	General Purpose Relativistic Atomic Structure Program
CIV3	The General Configuration Interaction Code
EUV	Extreme Ultraviolet
CSFs	Configuration State Functions
LSJ	Atomic Terms Symbol
a.u.	Atomic Units
Ry	Rydberg
f _l	Oscillator Strengths in Length Formulation
f _v	Oscillator Strengths in Velocity Formulation
A _l	Transition Probabilities in Length Formulation
A _v	Transition Probabilities in Velocity Formulation
E1	Electric Dipole Transition
E2	Electric Quadruple Transition
M1	Magnetic Dipole Transition

CHAPTER 1

INTRODUCTION

Magnesium is the eighth most abundant element in the earth crust, where it constitutes about 1.93 percent of the Earth primarily found in mineral deposits [1]. It has the ability to combine with other elements as it is never found in the pure form [2]. Magnesium was discovered in 1755 by Joseph Black [3]. It has an atomic number of 12, and its atomic weight is (24.304, 24.307) u [4]. Mg atom has ground state electron configuration of $1s^2 2s^2 2p^6 3s^2$ with twelve electrons. For our atomic system, Mg VII (Mg^{6+}) loses six electrons while keeping the components of the nucleus. Thus, the ground state electron configuration for Mg VII will be $1s^2 2s^2 2p^2$. We note that Mg VII is isoelectronic with carbon atom. Therefore, Mg VII is called carbon-like magnesium.

Carbon, nitrogen, and oxygen are the plentiful elements found in the universe and comprising the Earth's atmosphere they are also frequently observed in astrophysical objects. Emission lines of carbon like ions are beneficial for the studies of astrophysical plasmas, solar transition region, planetary nebulae, and fusion plasmas and precise atomic data are required for the interpretation of their spectra [5]. The National Aeronautics and Space Administration (NASA) space missions have been observing astrophysical objects spectra with high resolution in a broad wavelength region ranging from ultraviolet to X-ray. One of the recent experiments was flown on the Extreme Ultraviolet Explorer

spacecraft and on the Advanced X-Ray Astrophysical Facility. For stars, these spectra of high resolution can be obtained in X-ray wavelength and extreme ultraviolet wavelength ranges. For interpreting the large expected data from these missions, it is essential to have precise atomic data, for instance radiative decay rates and collision strengths for many cosmically abundant ions [6]. In planetary nebula NGC 7207, ultraviolet and infrared emission lines for Mg ions have also been observed [7].

Fractional abundances formed by magnesium are $\geq 1\%$ in charge state of Mg^{6+} in collisionally ionized plasmas (CPs) at specific electron temperature T_e with $k_B T_e$ in the range of 1.1–3.4 eV and photoionized plasmas (PPs) at $k_B T_e$ in the range of 27–104 eV, where k_B is Boltzman constant [8]. Among ground state configuration of Mg VII, a forbidden transition is of great importance regarding astrophysical applications providing information on composition, density and temperature from line intensity ratios and level populations. Mg VII ions constitute about 7.60 of solar corona on a scale of $\log n[\text{H}] = 12.0$. The ground state configuration of Mg VII $1s^2 2s^2 2p^2$ gives rise to 10 transitions: $^3P_0^e \Rightarrow ^3P_1^e$, $^3P_0^e \Rightarrow ^3P_2^e$, $^3P_1^e \Rightarrow ^3P_2^e$, $^3P_0^e \Rightarrow ^1D_2^e$, $^3P_1^e \Rightarrow ^1D_2^e$, $^3P_2^e \Rightarrow ^1D_2^e$, $^3P_0^e \Rightarrow ^1S_0^e$, $^3P_1^e \Rightarrow ^1S_0^e$, $^3P_2^e \Rightarrow ^1S_0^e$, $^1D_2^e \Rightarrow ^1S_0^e$, and these are called forbidden transitions. The significant transition that has been seen and identified in the EUV solar spectrum is $^3P_1^e \Rightarrow ^1S_0^e$ with wavelength 1189.82 Å [6]. Transition probabilities for the intercombination or semi-forbidden lines are found to be sensitive to the choice of wave functions and require sufficient justification of correlation and mixing effects. We have studied Mg VII oscillator strengths of different observed spectral features owing to Mg VII ions in this thesis.

Effects of configuration interaction are so prominent that even the most sophisticated calculations available for some transitions demonstrate strong disagreements. To determine the individual lines' strength, one of the critical factors is relativistic effect consideration for calculated data, particularly the term mixing of angular portion related to the wave functions. These effects significantly enhance across the periodic table horizontally. For highly excited atoms, LS coupling is usually less valid. With increasing nuclear charge (Z), the relativistic effects also become important. In intermediate coupling, individual line strengths have been computed by different theorists through the use of Breit-Pauli terms. These calculations are attributed to be computer intensive to variable degrees. As compared to emission experiments, these calculations sometimes result in larger deviations from LS coupling. The Opacity project is specifically limited to nonrelativistic multiplet data; LS-coupling scheme are applied for obtaining individual line data [9].

In the present study, various calculations regarding electric dipole transitions such as energy levels, transition probabilities, oscillator strengths and line strengths were investigated. The obtained results of calculations were used to compare with the data from Lestinsky et al. [8], Kelleher and Podobedova [9], NIST compilation [10], Bhatia and Doschek [11], Aggarwal [12], Froese Fischer and Tachiev [13], and Zhang and Sampson [14]. In the field of atomic computational atomic structure research study, one of the foremost contributors is Froese Fischer who developed the MCHF atomic structure codes. Computational methods such as MCHF and HF were used to evaluate different calculations in this thesis. Semi-relativistic MCHF code based on the Breit-Pauli

Hamiltonian has been used. This methodology uses the perturbation theory to include relativistic corrections. Our findings and computational results have been compared with other available results and are found in very well agreement except for a few transitions. As a result of cancellation effects, inconsistencies are specifically greater with weaker oscillator strengths of some semi-forbidden transitions.

CHAPTER 2

COMPUTATIONAL METHODS

In order to understand the atomic properties of Mg VII, we use two methods, first is called non-relativistic method and the second is called semi-relativistic method. Mg VII is a multi-electron ion with 6 electrons, where 2 electrons are in the 1s core-shell, and 4 electrons are outside the core. Because we have more than 1 electron, we have to apply an approximate method which helps us in solving the Schrödinger equation. Through this chapter, we will show two coupling schemes of calculations in depth and give an overview of the techniques applied.

2.1 Non-relativistic Method

The starting point of the calculations on many electron atoms is central field approximation, according to which it is assumed that each electron in a many electron complex atoms is acted upon by a central field produced by the nucleus which is assumed very small and infinitely heavy. This approximation holds because the deviation of the central potential $V(r)$ due to the close passage of all the other electrons is relatively small. This is so because the nuclear potential is larger than the effect of the above fluctuating potential.

Now in the case of two electron atoms, it is possible to treat the mutual interaction between the two electrons as a perturbation which is added to the central potential due to

the nucleus. To do the same in the case of the many electron atoms we have to write the unperturbed Hamiltonian so as to include the total effective central potential as stated above. The perturbation then contains the remaining spherical and all the non-spherical parts of the electronic interactions.

Now if the relativistic interaction, that is, perturbation is neglected then the central field Hamiltonian for the many electron systems can be written as [15]:

$$\mathcal{H} = \sum_{i=1}^N \left(-\frac{\hbar^2}{2m} \nabla_i^2 - \frac{Ze^2}{4\pi\epsilon_0 r_i} \right) + \sum_{i<j}^N \frac{e^2}{4\pi\epsilon_0 r_{ij}} \quad (1)$$

The symbol \mathcal{H} is known as the Hamiltonian operator of the atomic system. Z describes the atom's nuclear charge. Here r_i denotes the relative co-ordinate of the i^{th} electron with respect to the nucleus, $r_{ij} = |r_i - r_j|$, and the last summation is over all pairs of electrons. Now it is convenient to use atomic units so that the Hamiltonian becomes

$$\mathcal{H} = \sum_{i=1}^N \left(-\frac{1}{2} \nabla_i^2 - \frac{Z}{r_i} \right) + \sum_{i<j}^N \frac{1}{r_{ij}} \quad (2)$$

Now we can define any N-electron system using the wave function $\Psi(q_1, \dots, q_N)$ where $q_i = (r_i, \sigma_i)$ and r_i known as the space and σ_i known as the spin coordinates of the electron categorized i . The wave function Ψ is used to solve the time independent Schrödinger wave equation [16]

$$\mathcal{H}\Psi(q_1, \dots, q_N) = \Psi(q_1, \dots, q_N). \quad (3)$$

The symbol E is known as the eigenvalue of the Hamiltonian operator. The eigenvalue E refers to the overall energy of the system. The Eigen-function is the atomic state wave function $\Psi(q_1, \dots, q_N)$.

The Hamiltonian mentioned in the above equation is only accurate if it is assumed that the relativistic effects can be disregarded. Additionally, it is supposed that the nucleus is a point charge with a countless mass. The wave functions or eigenfunctions are described using

$$\psi(LS) = \sum_{i=1}^M a_i \phi_i(\alpha_i; LS). \quad (4)$$

Symbols L and S are the total orbital angular momentum and total spin angular momenta, M refers to number of the configurations and α_i refers to the angular momenta coupling scheme of the i^{th} configuration, a_i is the constant of normalization, and ϕ_i is the configuration state function. These wave functions are normalized:

$$\int_q |\psi(q_1, \dots, q_N)|^2 dq_1, \dots, dq_N \equiv \langle \psi | \psi \rangle = 1. \quad (5)$$

Taking into consideration that the integration is over all space and spin coordinates respectively, the approximate wave functions can be obtained by substituting the full Hamiltonian \mathcal{H} with a separable Hamiltonian which is given by

$$\mathcal{H} \approx \mathcal{H}_o = \sum_{i=1}^N \left(-\frac{1}{2} \nabla_i^2 - \frac{Z}{r_i} + V(r_i) \right), \quad (6)$$

where the potential $V(r_i)$ is an estimate for the Coulomb repulsion between the electrons.

The separable Hamiltonian like the full Hamiltonian commutes with the total angular momentum operators: L^2 , L_z , S^2 , and S_z . We can also select the wave functions of the separable Hamiltonian \mathcal{H}_0 to become the wave functions of these operators.

$$\mathcal{H}_0 \psi_0(q_1, \dots, q_N) = E_0 \psi_0(q_1, \dots, q_N). \quad (7)$$

We can write E_0 and ψ_0 as [14]: between the two electrons as a perturbation which is added to the central potential due to

$$E_0 = \sum_{i=1}^N E_i \quad (8)$$

$$\psi_0(q_1, \dots, q_N) = \prod_{i=1}^N \phi(\alpha_i; q_i). \quad (9)$$

Also, the 1-electron eigenfunction can be written as:

$$\phi(\alpha_i; q_i) = \frac{1}{r} P(nl; r) Y_{lm_l}(\theta, \varphi) X_{m_s}(\sigma), \quad (10)$$

where $P(nl; r)$ is radial eigenfunction, $Y_{lm_l}(\theta, \varphi)$ is the spherical harmonics, and n, l and m_l can assume the values

$$n = 1, 2, 3, \dots$$

$$l = 0, 1, 2, \dots, (n - 1)$$

$$m_l = 0, \pm 1, \pm 2, \dots, \pm l$$

When the spin of the electron is taken into account, each state of the electron is then characterized by the four quantum numbers n, l, m_l and m_s , where m_s can have values $\pm \frac{1}{2}$. The Hamiltonian \mathcal{H} does not change with respect the variations of electron coordinates. Accordingly, any variation of the coordinates in the product function leads to the wave function:

$$\Phi(q_1, \dots, q_N) = \mathcal{A} \prod_{i=1}^N \phi(\alpha_i; q_i) \quad (11)$$

Where \mathcal{A} refers to anti-symmetric function. We can express this function using the Slater determinant:

$$\Phi(q_1, \dots, q_N) = \frac{1}{\sqrt{N!}} \begin{vmatrix} \phi(\alpha_1; q_1) & \phi(\alpha_1; q_2) & \dots & \phi(\alpha_1; q_N) \\ \phi(\alpha_2; q_1) & \phi(\alpha_2; q_2) & \dots & \phi(\alpha_2; q_N) \\ \dots & \dots & \dots & \dots \\ \phi(\alpha_N; q_1) & \phi(\alpha_N; q_2) & \dots & \phi(\alpha_N; q_N) \end{vmatrix} \quad (12)$$

Since the determinant vanishes when two columns or rows are equal, we have the result that no two individual electrons can have all the four quantum numbers n, l, m_l and m_s equal. This is the statement of the Pauli exclusion principle. In the MCHF approach, the wave functions are estimated using a linear combination of orthonormal configuration state functions [16] given by

$$\Psi(\gamma LS) = \sum_{i=1}^M c_i \Phi(\gamma_i LS) \quad (13)$$

$$\sum_{i=1}^M c_i^2 = 1 \quad (14)$$

2.2. Semi-relativistic Method

To calculate the relativistic impact in atomic system Mg VII, we apply the Breit-Pauli Hamiltonian to correct our nonrelativistic Hamiltonian. The Breit-Pauli Hamiltonian is specified by [16]

$$\mathcal{H}_{BP} = \mathcal{H}_{NR} + \mathcal{H}_{RS} + \mathcal{H}_{FS} \quad (15)$$

\mathcal{H}_{NR} refers to the nonrelativistic many-electron Hamiltonian. \mathcal{H}_{RS} refers to the relativistic shift operator, and these vary with L and S which is given by the equation

$$\mathcal{H}_{RS} = \mathcal{H}_{MC} + \mathcal{H}_{D1} + \mathcal{H}_{D2} + \mathcal{H}_{OO} + \mathcal{H}_{SSC} \quad (16)$$

Symbol \mathcal{H}_{MC} refers to the mass correction term and is given by

$$\mathcal{H}_{MC} = -\frac{\alpha^2}{8} \sum_{i=1}^N (\nabla_i^2) + \nabla_i^2 \quad (17)$$

\mathcal{H}_{D1} and \mathcal{H}_{D2} are the one and 2-body Darwin terms which are estimated by

$$\mathcal{H}_{D1} = -\frac{\alpha^2 Z}{8} \sum_{i=1}^N \nabla_i^2 \left(\frac{1}{r_i} \right), \quad (18)$$

and

$$\mathcal{H}_{D2} = \frac{\alpha^2}{4} \sum_{i<j}^N \nabla_i^2 \left(\frac{1}{r_{ij}} \right) \quad (19)$$

respectively.

Also, \mathcal{H}_{OO} is the orbit-orbit term which is given by

$$\mathcal{H}_{OO} = -\frac{\alpha^2}{2} \sum_{i<j}^N \left[\frac{p_i \cdot p_j}{r_{ij}} + \frac{r_{ij}(r_{ij} \cdot p_i)p_j}{r_{ij}^3} \right] \quad (20)$$

Lastly, \mathcal{H}_{SSC} refers to the spin-spin contact factor which can be estimated by

$$\mathcal{H}_{SSC} = -\frac{8\pi\alpha^2}{3} \sum_{i<j}^N (s_i \cdot s_j) \delta(r_i \cdot r_j) \quad (21)$$

The fine structure operator \mathcal{H}_{FS} define the interactions among the spin and orbital angular momenta of the system. Additionally, the \mathcal{H}_{FS} does not vary with L and S , but this operator only varies with the total angular momentum operator $J = L + S$ [16].

$$\mathcal{H}_{FS} = \mathcal{H}_{SO} + \mathcal{H}_{SOO} + \mathcal{H}_{SS} \quad (22)$$

Where \mathcal{H}_{SO} is the spin-orbit term that can be estimated by

$$\mathcal{H}_{SO} = \frac{\alpha^2 Z}{2} \sum_{i=1}^N \frac{1}{r_i^3} l_i \cdot s_i \quad (23)$$

\mathcal{H}_{SOO} is the spin-other-orbit term given by

$$\mathcal{H}_{SOO} = -\frac{\alpha^2}{2} \sum_{i<j}^N \frac{r_{ij} \times p_i}{r_{ij}^3} (s_i + 2s_j) \quad (24)$$

\mathcal{H}_{SS} is the spin-spin parameter and is given by

$$\mathcal{H}_{SS} = \alpha^2 \sum_{i < j}^N \frac{1}{r_{ij}^3} \left[s_i \cdot s_j - 3 \frac{(s_i \cdot r_{ij})(s_j \cdot r_{ij})}{r_{ij}^2} \right] \quad (25)$$

The Breit-Pauli wave functions should be written as a linear combination

$$\psi(\gamma JM_J) = \sum_{i=1}^M c_i \Phi(\gamma_i L_i S_i JM_J), \quad (26)$$

where every M single-configuration functions Φ is composed of 1-electron functions, γ describes the coupling of angular momenta of the electrons, and c_i is mixing coefficient.

$$\Phi(\gamma_i L_i S_i JM_J) = \sum_{M_L M_S} \langle LM_L SM_S | LSJM_J \rangle \Phi(\gamma LM_L SM_S) \quad (27)$$

LSJ coupled CSFs are noticed to be described as $(\gamma_i L_i S_i JM_J)$. CSFs have dissimilar LS terms which are included within the above expansion as L and S are not good quantum numbers. In the intermediate coupling, the wave equation is given by [16]

$$Hc = Ec \quad (28)$$

$$H_{ij} = \langle \gamma_i L_i S_i JM_J | \mathcal{H}_{BP} | \gamma_j L_j S_j JM_J \rangle \quad (29)$$

Starting from this point, we consider fine structure levels of the system. This assumption will assist in comprehending how the relativistic energy corrections come into play. When the expansion mentioned in equation (26) includes the relativistic terms, we can express the energy as follows [16]:

$$E = E_{NR} + E_{RS} + E_{FS} \quad (30)$$

The term E_{NR} describes the ordinary nonrelativistic energy

$$E_{NR} = \langle \gamma LSJM_J | \mathcal{H}_{NR} | \gamma LSJM_J \rangle, \quad (31)$$

and term E_{RS} describes the relativistic shift contribution to the correction of relativistic energy. Also, it stands for a shift of the nonrelativistic energy term E_{NR} as E_{RS} is independent of J and M_J . The relativistic shift operators only change with L and S :

$$E_{RS} = \langle \gamma LSJM_J | \mathcal{H}_{RS} | \gamma LSJM_J \rangle \quad (32)$$

E_{FS} is known as the contribution of fine structure correction to the relativistic energy

$$E_{FS} = \langle \gamma LSJM_J | \mathcal{H}_{FS} | \gamma LSJM_J \rangle \quad (33)$$

On the other hand, we can express the fine structure as follows:

$$E_{FS} = E_{SO} + E_{SOO} + E_{SS} \quad (34)$$

And terms: E_{SO} , E_{SOO} and E_{SS} are known as the energies related to the spin-orbit, spin-other-orbit and spin-spin operators, respectively [16]. The energy depends on the J quantum number leading to the splitting of the nonrelativistic LS term E_{NR} energy into the fine structure levels. Next, we show addition of angular momenta giving the probable values of J for known values of L and S .

$$|L - S|, |L - S| + 1, \dots, L + S - 1, L + S, \quad (35)$$

where the number of levels in the term is specified by the multiplicity $2S+1$ if $L \leq S$ and by $2L+1$ if $L < S$.

E_{SO} and E_{SOO} are the spin-orbit and spin-other-orbit terms respectively, and each is product of rank one and spatial tensor operators.

$$E_{SO} = \langle \gamma LSJM_J | \mathcal{H}_{SO} | \gamma LSJM_J \rangle \propto (-1)^{L+S+J} \left\{ \begin{matrix} L & L & 1 \\ S & S & J \end{matrix} \right\} \quad (36)$$

$$E_{SOO} = \langle \gamma LSJM_J | \mathcal{H}_{SOO} | \gamma LSJM_J \rangle \propto (-1)^{L+S+J} \left\{ \begin{matrix} L & L & 1 \\ S & S & J \end{matrix} \right\} \quad (37)$$

Based on the concept of the Wigner Eckart [16] in addition to knowing that energy from the spin-spin operator is a scalar product of 2 rank and 2 tensor operators E_{SS} is as follows:

$$E_{SS} = \langle \gamma LSJM_J | \mathcal{H}_{SS} | \gamma LSJM_J \rangle \propto (-1)^{L+S+J} \left\{ \begin{matrix} L & L & 2 \\ S & S & J \end{matrix} \right\} \quad (38)$$

Referring to the expressions explicitly in 6-j symbols we get:

$$(-1)^{L+S+J} \left\{ \begin{matrix} L & L & 1 \\ S & S & J \end{matrix} \right\} \propto J(J+1) - L(L+1) - S(S+1) \quad (39)$$

$$(-1)^{L+S+J} \left\{ \begin{matrix} L & L & 2 \\ S & S & J \end{matrix} \right\} \propto \frac{3}{4} C(C+1) - L(L+1) - S(S+1) \quad (40)$$

And assume $C=J(J+1) - L(L+1) - S(S+1)$, hence we can write the fine-structure energies as follows:

$$E_{SO} = \{J(J+1) - L(L+1) - S(S+1)\} \zeta_{SO}(\gamma LS) \quad (41)$$

$$E_{SOO} = \{J(J + 1) - L(L + 1) - S(S + 1)\}\zeta_{SOO}(\gamma LS) \quad (42)$$

$$E_{SS} = \{J(J + 1) - L(L + 1) - S(S + 1)\}\zeta_{SS}(\gamma LS) \quad (43)$$

And $\zeta_{SO}(\gamma LS)$, $\zeta_{SOO}(\gamma LS)$ and $\zeta_{SS}(\gamma LS)$ are each independent on J.

Ignoring the spin-spin term leads to the energy difference between two sequential fine structure levels J and J-1

$$\Delta E_{FS} = 2\zeta J, \quad (44)$$

and the symbol ζ refers to the rule of Landé interval for the fine-structure and is given by

$$\zeta = \zeta_{SO}(\gamma LS) + \zeta_{SOO}(\gamma LS), \quad (45)$$

where the fine structure may be either normal or inverted. It is normal when it is positive, and the fine structure energy rises as the value of J increases. When it is negative, we say that the fine structure is inverted [16]. When the spin-spin term can't be ignored the rule of Landé interval breaks down, and the fine structure shows unbalanced behavior. This behavior is noticed when dissimilar CSFs with dissimilar L and S, where each one couples to the same total J, are involved in the equation [16]. Figure 1 shows an example of the fine structure and term splitting of the $1s^2 2s^2 2p^2$ configuration in our proposed Mg VII system.

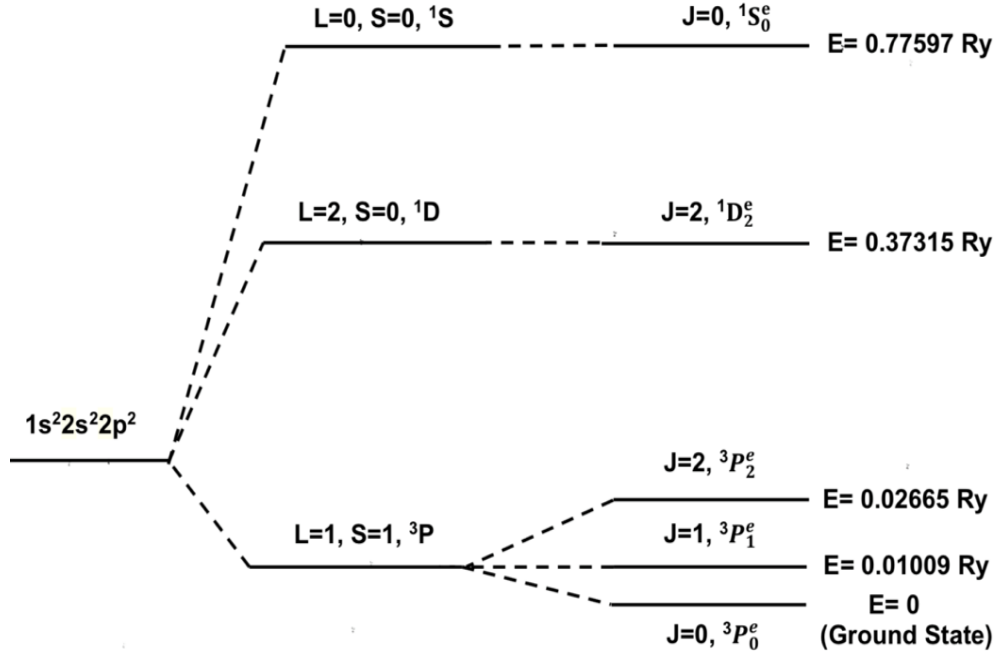


FIG. 1. The fine-structure and term splitting of the $1s^2 2s^2 2p^2$ configuration in Mg VII.

In the Breit-Pauli calculations, we have ignored the spin-spin, orbit-orbit, and second Darwin contact terms. The eigenfunctions from equation (6) can be used to describe the length and velocity structures of the oscillator strengths and transition possibilities for transitions between the fine structure levels. The oscillator strengths can be indicated as absorption or emission oscillator strength. We can write the absorption oscillator strengths as:

$$f^{\pi k}(\gamma J, \gamma' J') = \frac{1}{\alpha} C_k [\alpha (E_{\gamma' J'} - E_{\gamma J})]^{2k-1} \frac{S^{\pi k}(\gamma J, \gamma' J')}{g_J}, \quad (46)$$

where the atom in the lower state absorbs a photon, then it is excited to an upper state.

Here $g_{J'}$ is the statistical weight of the upper level which can be written as:

$$g_{J'} = 2J' + 1, \quad (47)$$

And

$$C_k = \frac{(2k+1)(k+1)}{k((2k+1)!!)^2} \quad (48)$$

$S^{\pi k}(\gamma J, \gamma' J')$ refers to the line strength given by

$$S^{\pi k}(\gamma J, \gamma' J') = \sum_{M, M', q} \left| \langle \gamma J M | O_q^{\pi(k)} | \alpha' J' M' \rangle \right|^2 \quad (49)$$

Where $O_q^{\pi(k)}$ is a general transition operator of rank k and parity π . For electric multi-pole transition ($\pi = (-1)^k$) and magnetic multi-pole transition ($\pi = (-1)^{k+1}$) the electric multi-pole transition operator is calculated by

$$E_q^{(k)} = \sum_{i=1}^N r^{k(i)} C_q^{(k)}(i), \quad (50)$$

and the magnetic multi-pole transition operator is given by

$$M_q^{(k)} = \alpha \sqrt{k(2k+1)} \left[\frac{1}{k+1} M A_q^{(k)} + \frac{1}{2} g_s M B_q^{(k)} \right] \quad (51)$$

$$M A_q^{(k)} = \sum_{i=1}^N r^{k-1}(i) [c^{(k-1)}(i) \times L^{(1)}(i)]_q^{(k)} \quad (52)$$

$$M B_q^{(k)} = \sum_{i=1}^N r^{k-1}(i) [c^{(k-1)}(i) \times S^{(1)}(i)]_q^{(k)} \quad (53)$$

We begin with the transition integral to comprehend how the transition happens among an upper state and a lower state

$$L_q^{\pi k}(\gamma JM, \gamma' J' M') = \langle \gamma JM | O_q^{\pi(k)} | \gamma' J' M' \rangle, \quad (54)$$

and the component strength is given as follows:

$$S^{\pi k}(\gamma JM, \gamma' J' M') = \sum_q |L_q^{\pi k}(\gamma JM, \gamma' J' M')|^2 \quad (55)$$

Furthermore, the transition possibility from the upper level to the lower level can be calculated by

$$A^{\pi k}(\gamma J, \gamma' J') = 2C_k [\alpha(E_{\gamma' J'} - E_{\gamma J})]^{2k+1} \frac{S^{\pi k}(\gamma J, \gamma' J')}{g_{J'}}, \quad (56)$$

where the lifetime, $\tau_{\gamma' J'}$ is opposite of the summation of transition possibilities over the multi-pole transitions to every lower energy level [16-17]:

$$\tau_{\gamma' J'} = \frac{1}{\sum_{\pi k, \gamma J} A^{\pi k}(\gamma J, \gamma' J')} \quad (57)$$

CHAPTER 3

RESULTS AND DISCUSSION

3.1 Energy levels

In Table I, we have presented the first fifty-two (52) energy levels of Mg VII arising from the $(1s^2)2s^22p^2$, $2s2p^3$, $2p^4$, $2s^22p3s$, $2s^22p3p$, $2s2p^2(^4P)3s$ and $2s^22p3d$ configurations, and we have compared our calculated energies with NIST compilation [10]. In the same table we have also compared our results with the theoretical level energies of Bhatia and Doschek [11] obtained using the SS program of Eissner et al. (1974) Aggarwal [12] who used the CIV3 code of Hibbert (1975), Froese Fischer and Tachiev [13] obtained from the MCHF method and also Zhang and Sampson [14] who used the GRASP program of Dyall et al. (1989). We note that the NIST results are available only for the 42 energy levels; thus, the NIST values are not available for 10 levels. These levels are $2s^22p3p\ ^1P_1^e$, $2s^22p3p\ ^3D_1^e$, $2s^22p3p\ ^3D_2^e$, $2s^22p3p\ ^3D_3^e$, $2s^22p3p\ ^3S_1^e$, $2s^22p3p\ ^1D_2^e$, $2s^22p3p\ ^1S_0^e$, $2s2p^2(^4P)3s\ ^3P_1^e$, $2s^22p3d\ ^3F_3^o$ and $2s^22p3d\ ^3F_4^o$. Furthermore, we observe that the other theoretical results are computed for 46 energy levels, thus we note that six energy levels computed in the present work were not given in the other theoretical results. These levels are $2s2p^2(^4P)3s\ ^3P_1^e$, $2s2p^2(^4P)3s\ ^5P_2^e$, $2s2p^2(^4P)3s\ ^5P_3^e$, $2s2p^2(^4P)3s\ ^3P_0^e$, $2s2p^2(^4P)3s\ ^3P_1^e$ and $2s2p^2(^4P)3s\ ^3P_2^e$.

TABLE I. Comparison of present excited energy levels of Mg VII (Ry) with NIST compilation and other theoretical calculations.

Index	CFS	LSJ	Energy Levels (Ry)						
			Present	[NIST]	[MCHF]	[SS]	[CIV3]	[GRASP]	[Diff]
1.	$2s^2 2p^2$	$^3P_0^e$	0.0000	0.0000	0.0000	0.0000	0.0000	0.0000	0.0000
2.		$^3P_1^e$	0.0101	0.0101	0.0102	0.0102	0.0099	0.0105	0.0000
3.		$^3P_2^e$	0.0280	0.0267	0.0268	0.0269	0.0262	0.0276	0.0013
4.	$2s^2 2p^2$	$^1D_2^e$	0.3827	0.3732	0.3742	0.3964	0.4018	0.3935	0.0095
5.	$2s^2 2p^2$	$^1S_0^e$	0.7922	0.7760	0.7758	0.7427	0.8440	0.7426	0.0162
6.	$2s 2p^3$	$^5S_2^o$	1.0655	1.0760	1.0998	0.9682	1.0508	0.9703	-0.0105
7.	$2s 2p^3$	$^3D_3^o$	2.1347	2.1219	2.1476	2.1309	2.1456	2.1429	0.0128
8.		$^3D_2^o$	2.1340	2.1229	2.1486	2.1302	2.1465	2.1437	0.0111
9.		$^3D_1^o$	2.1340	2.1235	2.1492	2.1303	2.1469	2.1441	0.0105
10.	$2s 2p^3$	$^3P_1^o$	2.5241	2.5051	2.5314	2.5083	2.5521	2.5191	0.0190
11.		$^3P_2^o$	2.5248	2.5051	2.5315	2.5087	2.5525	2.5198	0.0197
12.		$^3P_0^o$	2.5238	2.5055	2.5319	2.5080	2.5527	2.5192	0.0183
13.	$2s 2p^3$	$^1D_2^e$	3.2633	3.2295	3.2569	3.3594	3.2886	3.3691	0.0338
14.	$2s 2p^3$	$^3S_1^o$	3.3337	3.2999	3.3264	3.4295	3.3456	3.4203	0.0338
15.	$2s 2p^3$	$^1P_1^o$	3.6609	3.6191	3.6472	3.7380	3.7054	3.7451	0.0418
16.	$2p^4$	$^3P_2^e$	4.9787	4.9420	4.9397	5.0547	5.0430	5.0547	0.0367
17.		$^3P_1^e$	4.9966	4.9609	4.9586	5.0736	5.0615	5.0726	0.0357
18.		$^3P_0^e$	5.0047	4.9688	4.9665	5.0821	5.0693	5.0802	0.0359
14.	$2s 2p^3$	$^3S_1^o$	3.3337	3.2999	3.3264	3.4295	3.3456	3.4203	0.0338
20.	$2p^4$	$^1S_0^e$	6.0616	6.0001	6.0019	6.2169	6.1798	6.2152	0.0615
21.	$2s^2 2p 3s$	$^3P_0^o$	9.5700	9.5465	9.5668	9.7153	9.6067	9.4284	0.0235
22.		$^3P_1^o$	9.5782	9.5537	9.5748	9.7233	9.6143	9.4365	0.0245

TABLE I. (*Continued*).

Index	CFS	LSJ	Energy Levels (Ry)						
			Present	[NIST]	[MCHF]	[SS]	[CIV3]	[GRASP]	[Diff]
23.		$^3P_2^o$	9.5997	9.5764	9.5963	9.7437	9.6336	9.4585	0.0233
24.	$2s^22p3s$	$^1P_1^o$	9.6933	9.6688	9.6902	9.8430	9.7485	9.5556	0.0245
25.	$2s^22p3p$	$^1P_1^e$	10.0944	-	10.0830	10.2295	10.0853	9.9081	-
26.	$2s^22p3p$	$^3D_1^e$	10.1445	-	10.1368	10.2687	10.1428	9.9558	-
27.		$^3D_2^e$	10.1536	-	10.1460	10.2770	10.1517	9.9654	-
28.		$^3D_3^e$	10.1723	-	10.1646	10.2948	10.1689	9.9852	-
29.	$2s^22p3p$	$^3S_1^e$	10.2302	-	10.2258	10.3583	10.2336	10.0426	-
30.	$2s^22p3p$	$^3P_0^e$	10.2675	10.2403	10.2671	10.4720	10.2828	10.0727	0.0272
31.		$^3P_1^e$	10.2764	10.2512	10.2758	10.4793	10.2903	10.0823	0.0252
32.		$^3P_2^e$	10.2865	10.2594	10.2855	10.4896	10.2995	10.0918	0.0271
33.	$2s^22p3p$	$^1D_2^e$	10.4504	-	10.4454	10.6124	10.4818	10.2653	-
34.	$2s^22p3p$	$^1S_0^e$	10.6545	-	10.6349	10.8075	10.6824	10.4615	-
35.	$2s2p^2(^4P)3s$	$^5P_1^e$	10.7605	-	-	-	-	-	-
36.	$2s^22p3d$	$^3F_2^o$	10.7745	10.7416	10.7643	10.8946	10.7472	10.6558	0.0329
37.	$2s2p^2(^4P)3s$	$^5P_2^e$	10.7707	10.7526	-	-	-	-	0.0181
38.	$2s2p^2(^4P)3s$	$^5P_3^e$	10.7857	10.7661	-	-	-	-	0.0196
39.	$2s^22p3d$	$^3F_3^o$	10.7922	-	10.7808	10.9081	10.7643	10.6588	-
40.	$2s^22p3d$	$^1D_2^o$	10.7938	10.7612	10.7840	10.9202	10.7647	10.6345	0.0326
41.	$2s^22p3d$	$^3F_4^o$	10.8073	-	10.7956	10.9224	10.7777	10.6757	-
42.	$2s^22p3d$	$^3D_1^o$	10.8969	10.8600	10.8826	11.0301	10.8767	10.7470	0.0369
43.		$^3D_2^o$	10.9006	10.8639	10.8863	11.0332	10.8796	10.7506	0.0367
44.		$^3D_3^o$	10.9095	10.8719	10.8946	11.0418	10.8875	10.7595	0.0376
45.	$2s^22p3d$	$^3P_2^o$	10.9399	10.9056	10.9278	11.0683	10.9144	10.7925	0.0343

TABLE I. (*Continued*).

Index	CFS	LSJ	Energy Levels (Ry)						
			Present	[NIST]	[MCHF]	[SS]	[CIV3]	[GRASP]	[Diff]
46.		$^3P_1^o$	10.9461	10.9120	10.9346	11.0742	10.9204	10.7992	0.0341
47.		$^3P_0^o$	10.9492	10.9156	10.9384	11.0771	10.9237	10.8028	0.0336
48.	$2s2p^2(^4P)3s$	$^3P_0^e$	11.0789	11.0369	-	-	-	-	0.0420
49.	$2s^22p3d$	$^1F_3^e$	11.0977	11.0428	11.0660	11.2459	11.0881	10.9697	0.0549
50.	$2s2p^2(^4P)3s$	$^3P_1^e$	11.0872	11.0448	-	-	-	-	0.0424
51.	$2s^22p3d$	$^1P_1^o$	11.1001	11.0518	11.0750	11.2419	11.0897	10.9594	0.0483
52.	$2s2p^2(^4P)3s$	$^3P_2^e$	11.1034	11.0598	-	-	-	-	0.0436

[NIST] Kramida, Ralchenko, Reader and NIST ASD Team [10].

[MCHF] Froese Fischer and Tachiev [13].

[SS] Bhatia and Doschek, [11].

[CIV3] Aggarwal [12].

[GRASP] Zhang and Sampson [14].

[Diff] Difference between the present calculation and NIST compilation.

The agreement of the present calculated energies with the NIST and other calculated energies is excellent. The average deviation is of around 0.025 Ry for all levels, with the exceptions of the $2p^4 \ ^1S_0^e$ and $2s^22p3d \ ^1F_3^e$ levels that deviate around 0.0615 Ry and 0.0549 Ry, respectively from the NIST values. We have also found difference for the $2s2p^3 \ ^5S_2^o$ level where the present value is lower than the NIST compilation by around 0.0105 Ry. The present values agree very well with the NIST results for the first twelve (12) energy levels. The present results also agree very well with the MCHF calculations of Froese Fischer and Tachiev for all levels. The average deviation is of around 0.0077 Ry, with the exception of the $2p^4 \ ^1D_2^e$ and $2p^4 \ ^1S_0^e$ levels that

deviate by 0.0445 Ry and 0.0597 Ry, respectively. The present results agree very well with Froese Fischer and Tachiev results for the $2s^22p^2\ ^3P_1^e$, $2s^22p3p\ ^3P_0^e$, $2s^22p3p\ ^3P_1^e$ and $2s^22p3p\ ^3P_2^e$ levels with deviation of 0.0001 Ry, 0.0004 Ry, 0.0006 Ry and 0.0010 Ry, respectively. As seen from the table, our MCHF calculation displays slightly better agreement with the MCHF results of Froese Fischer and Tachiev calculation.

For the SS and GRASP calculations, the agreement is similar among the results for the lowest 20 levels, with average deviation of around 0.0038 Ry. Therefore, the agreement of the present calculated energies with the SS and GRASP calculated energies is good with the first twelve (12) levels, with the exception of the $2s2p^3\ ^5S_2^o$ with deviation of 0.0962 Ry. The agreement among the SS energy levels and NIST results are better in seven levels from the first 12 levels. On the other hand, the present energies are in better agreement with the NIST results, particularly for the last 25 levels for which the SS energy levels are consistently higher. Likewise, the agreement among the GRASP energy levels and NIST results are better in four levels from the first 12 levels. However, the present energies are in better agreement with the NIST results, especially for the last 17 levels for which the GRASP energy levels are consistently lower.

The present results generally agree with the CIV3 calculation for most levels. The present results agree very well with the CIV3 results for the $2s^22p^2\ ^3P_1^e$, $2s^22p3p\ ^1P_1^e$, $2s^22p3p\ ^3D_1^e$, $2s^22p3p\ ^3D_2^e$, $2s^22p3p\ ^3D_3^e$, and $2s^22p3p\ ^3S_1^e$, with average deviation of around 0.00214 Ry. The CIV3 energies for the last ten levels are in better agreement with NIST results, whereas the present energy levels are much closer of the NIST energy levels for most of the first 27 levels for which the CIV3 energy levels are higher.

3.2 Lifetimes

We have calculated transition probabilities of transitions between the levels of the ground configuration $(1s^2)2s^22p^2$ and the excited configurations $2s2p^3$, $2p^4$, $2s^22p3s$, $2s^22p3p$, $2s2p^2(^4P)3s$ and $2s^22p3d$. In Table II, we have listed the lifetimes and compared them with Lestinsky et al. [8] and Froese Fischer and Tachiev [13]. As seen from the table that some transitions calculated in the present work were not given in the other theoretical results. The agreement of our lifetimes results with the other two theoretical results is excellent. The present lifetimes agree very well with Froese Fischer and Tachiev for all levels, especially very good agreement for the $2s^22p^2\ ^1D_2^e$, $2s2p^3\ ^1P_1^o$, $2s^22p3p\ ^3P_0^e$, $2s^22p3p\ ^3P_1^e$ and $2s^22p3p\ ^3P_2^e$ levels. We note from this table that Mg VII has some long-lived metastable levels: $2s^22p^2\ ^3P_1^e$, $2s^22p^2\ ^3P_2^e$, $2s^22p^2\ ^1D_2^e$, $2s^22p^2\ ^1S_0^e$, and $2s2p^3\ ^5S_2^o$. These five levels have considerably higher lifetimes than the other levels. This is because the transitions between these four levels are not allowed transitions; they are forbidden transitions, and the transition to the fifth level is called semi-forbidden or intercombination transition. On the other hand, the remaining transitions are allowed transitions.

TABLE II. Comparison of lifetimes (s) of Mg VII levels with other calculations.

Index	CFS	LSJ	Lifetimes (s)		
			Present	[CFF]	[L]
1.	$2s^22p^2$	$^3P_0^e$	0	0	0
2.		$^3P_1^e$	4.14E+01	3.93E+01	3.89E+01
3.		$^3P_2^e$	1.27E+01	1.25E+01	1.20E+01

TABLE II. (Continued).

Index	CFS	LSJ	Lifetimes (s)		
			Present	[CFF]	[L]
4.	$2s^22p^2$	$^1D_2^e$	2.23E-01	2.24E-01	2.04E-01
5.	$2s^22p^2$	$^1S_0^e$	2.63E-02	2.44E-02	2.38E-02
6.	$2s2p^3$	$^5S_2^o$	2.15E-05	1.87E-05	2.27E-05
7.	$2s2p^3$	$^3D_2^o$	5.80E-10	5.64E-10	5.13E-10
8.		$^3D_1^o$	5.72E-10	5.55E-10	5.06E-10
9.		$^3D_3^o$	5.94E-10	5.78E-10	5.26E-10
10.	$2s2p^3$	$^3P_0^o$	2.16E-10	2.13E-10	1.02E-10
11.		$^3P_1^o$	2.18E-10	2.14E-10	1.93E-10
12.		$^3P_2^o$	2.20E-10	2.17E-10	1.95E-10
13.	$2s2p^3$	$^1D_2^o$	7.22E-11	7.19E-11	6.41E-11
14.	$2s2p^3$	$^3S_1^o$	3.36E-11	3.38E-11	3.10E-11
15.	$2s2p^3$	$^1P_1^o$	4.35E-11	4.36E-11	3.86E-11
16.	$2p^4$	$^3P_2^e$	6.27E-11	6.65E-11	5.56E-11
17.		$^3P_1^e$	6.22E-11	6.60E-11	5.52E-11
18.		$^3P_0^e$	6.20E-11	6.58E-11	5.51E-11
19.	$2p^4$	$^1D_2^e$	1.28E-10	1.36E-10	1.10E-10
20.	$2p^4$	$^1S_0^e$	5.47E-11	5.80E-11	4.67E-11
21.	$2s^22p3s$	$^3P_0^o$	1.98E-11	1.92E-11	-
22.		$^3P_1^o$	1.95E-11	1.90E-11	-
23.		$^3P_2^o$	1.97E-11	1.90E-11	-
24.	$2s^22p3s$	$^1P_1^o$	1.19E-11	1.22E-11	-
25.	$2s^22p3p$	$^1P_1^e$	6.04E-10	6.77E-10	-
26.	$2s^22p3p$	$^3D_1^e$	5.37E-10	6.04E-10	-

TABLE II. (Continued).

Index	CFS	LSJ	Lifetimes (s)		
			Present	[CFF]	[L]
27.		${}^3D_2^e$	5.33E-10	6.00E-10	-
28.		${}^3D_3^e$	5.34E-10	6.01E-10	-
29.	$2s^22p3p$	${}^1S_1^e$	1.88E-10	2.00E-10	-
30.	$2s^22p3p$	${}^3P_0^e$	1.32E-10	1.33E-10	-
31.		${}^3P_1^e$	1.34E-10	1.35E-10	-
32.		${}^3P_2^e$	1.33E-10	1.34E-10	-
33.	$2s^22p3p$	${}^1D_2^e$	3.61E-10	4.05E-10	-
34.	$2s^22p3p$	${}^1S_0^e$	1.52E-10	1.78E-10	-
35.	$2s2p^2({}^4P)3s$	${}^5P_1^e$	2.58E-11	-	-
36.		${}^5P_2^e$	2.56E-11	-	-
37.	$2s^22p3d$	${}^3F_2^o$	1.43E-11	1.64E-11	-
38.	$2s2p^2({}^4P)3s$	${}^5P_3^e$	2.53E-11	-	-
39.	$2s^22p3d$	${}^3F_3^o$	2.49E-10	2.40E-10	-
40.	$2s^22p3d$	${}^1D_2^o$	9.65E-12	8.98E-12	-
41.	$2s^22p3d$	${}^3F_4^o$	2.18E-09	2.27E-09	-
42.	$2s^22p3d$	${}^3D_1^o$	2.24E-12	2.27E-12	-
43.		${}^3D_2^o$	2.31E-12	2.33E-12	-
44.		${}^3D_3^o$	2.22E-12	2.26E-12	-
45.	$2s^22p3d$	${}^3P_2^o$	3.69E-12	3.78E-12	-
46.		${}^3P_1^o$	3.81E-12	3.88E-12	-
47.		${}^3P_0^o$	3.91E-12	3.96E-12	-
48.	$2s2p^2({}^4P)3s$	${}^3P_0^e$	1.42E-11	-	-
49.		${}^3P_1^e$	1.41E-11	-	-

TABLE II. (Continued).

Index	CFS	LSJ	Lifetimes (s)		
			Present	[CFF]	[L]
50.	2s ² 2p3d	¹ F ₃ ^e	1.83E-12	1.95E-12	-
51.	2s ² 2p3d	¹ P ₁ ^o	2.93E-12	3.17E-12	-
52.	2s2p ² (⁴ P)3s	³ P ₂ ^e	1.41E-11	-	-

[CFF] Froese Fischer and Tachiev [13].

[L] Lestinsky et al. [8].

3.3 Oscillator Strengths and Transition Probabilities

3.3.1 Oscillator Strengths and Transition Probabilities for Some E1 Transitions

In Table III, we have made a comparison of the length values of oscillator strengths and transition probabilities for some E1 transitions among the terms of the ground (1s²)2s²2p² and the excited 2s2p³, 2s²2p3s, and 2s²2p3d configurations. Included in this table are the results of Kelleher and Podobedova [9] calculation, along with our present results. We have shown in the table that g_i and g_k , where g_i is the statistical weight of the initial (lower) state, can be calculated by $(2J_i+1)$. The g_k is the statistical weight of the final (upper) state. Likewise, it can be calculated by $(2J_k+1)$. Here, J means Total Angular Momentum Quantum Number.

TABLE III. Comparison of present oscillator strengths and transition probabilities (s^{-1}) for some E1 transitions in Mg VII with DEK results.

Transition				Present				[DEK]	
Initial Level	Final Level	g_i	g_k	f_l	A_l	f_l	A_l		
$2s^22p^2$	$3p_e$	$2s2p^3$	$5S_o$	3	5	2.35E-06	1.26E+04	2.52E-06	1.38E+04
$2s^22p^2$	$3p_e$	$2s2p^3$	$5S_o$	5	5	3.93E-06	3.40E+04	3.82E-06	3.38E+04
$2s^22p^2$	$3p_e$	$2s2p^3$	$3D_o$	1	3	8.50E-02	1.04E+09	8.50E-02	1.03E+09
$2s^22p^2$	$3p_e$	$2s2p^3$	$3D_o$	3	3	1.87E-02	6.78E+08	1.88E-02	6.73E+08
$2s^22p^2$	$3p_e$	$2s2p^3$	$3D_o$	3	5	6.32E-02	1.37E+09	6.32E-02	1.36E+09
$2s^22p^2$	$3p_e$	$2s2p^3$	$3D_o$	5	3	5.81E-04	3.45E+07	5.88E-04	3.46E+09
$2s^22p^2$	$3p_e$	$2s2p^3$	$3D_o$	5	5	9.78E-03	3.48E+08	9.84E-03	3.47E+08
$2s^22p^2$	$3p_e$	$2s2p^3$	$3D_o$	5	7	6.60E-02	1.68E+09	6.61E-02	1.67E+09
$2s^22p^2$	$3p_e$	$2s2p^3$	$3p_o$	1	3	8.77E-02	1.50E+09	8.83E-02	1.48E+09
$2s^22p^2$	$3p_e$	$2s2p^3$	$3p_o$	3	1	3.03E-02	4.62E+09	3.03E-02	4.54E+09
$2s^22p^2$	$3p_e$	$2s2p^3$	$3p_o$	3	3	2.53E-02	1.29E+09	2.54E-02	1.27E+09
$2s^22p^2$	$3p_e$	$2s2p^3$	$3p_o$	3	5	3.37E-02	1.03E+09	3.40E-02	1.02E+09
$2s^22p^2$	$3p_e$	$2s2p^3$	$3p_o$	5	3	2.17E-02	1.81E+09	2.19E-02	1.80E+09
$2s^22p^2$	$3p_e$	$2s2p^3$	$3p_o$	5	5	7.02E-02	3.52E+09	7.06E-02	3.48E+09
$2s^22p^2$	$3p_e$	$2s2p^3$	$1D_o$	3	5	1.58E-05	8.05E+05	1.42E-05	7.05E+05
$2s^22p^2$	$3p_e$	$2s2p^3$	$1D_o$	5	5	1.67E-04	1.40E+07	1.62E-04	1.34E+07
$2s^22p^2$	$3p_e$	$2s2p^3$	$3S_o$	1	3	1.10E-01	3.29E+09	1.10E-01	3.21E+09
$2s^22p^2$	$3p_e$	$2s2p^3$	$3S_o$	3	3	1.11E-01	9.87E+09	1.11E-01	9.66E+09
$2s^22p^2$	$3p_e$	$2s2p^3$	$3S_o$	5	3	1.14E-01	1.66E+10	1.13E-01	1.63E+10

TABLE III. (Continued).

Transition				Present				[DEK]	
Initial Level	Final Level	g_i	g_k	f_1	A_1	f_1	A_1		
$2s^22p^2$	$3p_e$	$2s2p^3$	$1p_o$	1	3	5.60E-06	2.01E+05	4.17E-06	1.46E+05
$2s^22p^2$	$3p_e$	$2s2p^3$	$1p_o$	3	3	1.99E-04	2.13E+07	1.81E-04	1.89E+07
$2s^22p^2$	$3p_e$	$2s2p^3$	$1p_o$	5	3	9.85E-06	1.74E+06	5.88E-06	1.02E+06
$2s^22p^2$	$3p_e$	$2s^22p3s$	$3p_o$	1	3	6.82E-02	1.68E+10	7.04E-02	1.73E+10
$2s^22p^2$	$3p_e$	$2s^22p3s$	$3p_o$	3	1	2.30E-02	5.06E+10	2.34E-02	5.13E+10
$2s^22p^2$	$3p_e$	$2s^22p3s$	$3p_o$	3	3	1.69E-02	1.24E+10	1.73E-02	1.27E+10
$2s^22p^2$	$3p_e$	$2s^22p3s$	$3p_o$	3	5	2.87E-02	1.27E+10	2.94E-02	1.30E+10
$2s^22p^2$	$3p_e$	$2s^22p3s$	$3p_o$	5	3	1.73E-02	2.12E+10	1.77E-02	2.14E+10
$2s^22p^2$	$3p_e$	$2s^22p3s$	$3p_o$	5	5	5.17E-02	3.81E+10	5.29E-02	3.88E+10
$2s^22p^2$	$3p_e$	$2s^22p3s$	$1p_o$	1	3	5.10E-04	1.28E+08	-	-
$2s^22p^2$	$3p_e$	$2s^22p3s$	$1p_o$	3	3	2.51E-04	1.89E+08	-	-
$2s^22p^2$	$3p_e$	$2s^22p3s$	$1p_o$	5	3	6.54E-05	8.18E+07	-	-
$2s^22p^2$	$3p_e$	$2s^22p3d$	$3F_o$	3	5	5.66E-05	3.16E+07	-	-
$2s^22p^2$	$3p_e$	$2s^22p3d$	$3F_o$	5	5	1.25E-03	1.16E+09	-	-
$2s^22p^2$	$3p_e$	$2s^22p3d$	$3F_o$	5	7	4.37E-03	2.91E+09	-	-
$2s^22p^2$	$3p_e$	$2s^22p3d$	$1D_o$	3	5	5.70E-03	3.19E+09	-	-
$2s^22p^2$	$3p_e$	$2s^22p3d$	$1D_o$	5	5	1.73E-04	1.61E+08	-	-
$2s^22p^2$	$3p_e$	$2s^22p3d$	$3D_o$	1	3	9.39E-01	2.98E+11	9.36E-01	2.96E+11
$2s^22p^2$	$3p_e$	$2s^22p3d$	$3D_o$	3	3	1.52E-01	1.45E+11	1.53E-01	1.44E+11
$2s^22p^2$	$3p_e$	$2s^22p3d$	$3D_o$	3	5	6.90E-01	3.94E+11	6.89E-01	3.91E+11
$2s^22p^2$	$3p_e$	$2s^22p3d$	$3D_o$	5	3	1.61E-03	2.55E+09	1.68E-03	2.64E+09

TABLE III. (Continued).

Transition				Present				[DEK]	
Initial Level	Final Level	g_i	g_k	f_1	A_1	f_1	A_1		
$2s^22p^2$	$3p_e$ $2s^22p3d$	$3D_o$	5	5	4.09E-02	3.88E+10	4.15E-02	3.92E+10	
$2s^22p^2$	$3p_e$ $2s^22p3d$	$3D_o$	5	7	6.61E-01	4.49E+11	6.61E-01	4.46E+11	
$2s^22p^2$	$3p_e$ $2s^22p3d$	$3p_o$	1	3	1.17E-01	3.76E+10	1.21E-01	3.85E+10	
$2s^22p^2$	$3p_e$ $2s^22p3d$	$3p_o$	3	1	8.85E-02	2.55E+11	8.92E-02	2.56E+11	
$2s^22p^2$	$3p_e$ $2s^22p3d$	$3p_o$	3	3	1.13E-01	1.08E+11	1.12E-01	1.07E+11	
$2s^22p^2$	$3p_e$ $2s^22p3d$	$3p_o$	3	5	8.91E-03	5.13E+09	9.73E-03	5.56E+09	
$2s^22p^2$	$3p_e$ $2s^22p3d$	$3p_o$	5	3	7.25E-02	1.16E+11	7.30E-02	1.16E+11	
$2s^22p^2$	$3p_e$ $2s^22p3d$	$3p_o$	5	5	2.75E-01	2.63E+11	2.76E-01	2.62E+11	
$2s^22p^2$	$3p_e$ $2s^22p3d$	$1F_o$	5	7	4.40E-06	3.09E+06	-	-	
$2s^22p^2$	$3p_e$ $2s^22p3d$	$1p_o$	1	3	1.77E-03	5.84E+08	-	-	
$2s^22p^2$	$3p_e$ $2s^22p3d$	$1p_o$	3	3	2.46E-04	2.43E+08	-	-	
$2s^22p^2$	$3p_e$ $2s^22p3d$	$1p_o$	5	3	1.49E-05	2.44E+07	-	-	
$2s^22p^2$	$1D_e$ $2s2p^3$	$5S_o$	5	5	1.96E-09	7.33E+00	-	-	
$2s^22p^2$	$1D_e$ $2s2p^3$	$3D_o$	5	3	3.79E-06	1.56E+05	3.76E-06	1.54E+05	
$2s^22p^2$	$1D_e$ $2s2p^3$	$3D_o$	5	5	1.10E-05	2.72E+05	9.75E-06	2.40E+05	
$2s^22p^2$	$1D_e$ $2s2p^3$	$3D_o$	5	7	6.74E-05	1.19E+06	6.81E-05	1.20E+06	
$2s^22p^2$	$1D_e$ $2s2p^3$	$3p_o$	5	3	2.33E-05	1.43E+06	2.37E-05	1.44E+06	
$2s^22p^2$	$1D_e$ $2s2p^3$	$3p_o$	5	5	5.27E-06	1.94E+05	5.16E-06	1.89E+05	
$2s^22p^2$	$1D_e$ $2s2p^3$	$1D_o$	5	5	2.07E-01	1.38E+10	2.07E-01	1.36E+10	
$2s^22p^2$	$1D_e$ $2s2p^3$	$3S_o$	5	3	1.80E-05	2.10E+06	1.33E-05	1.53E+06	
$2s^22p^2$	$1D_e$ $2s2p^3$	$1p_o$	5	3	1.28E-01	1.84E+10	1.29E-01	1.82E+10	

TABLE III. (Continued).

Transition				Present				[DEK]	
Initial Level	Final Level	g_i	g_k	f_1	A_1	f_1	A_1		
$2s^2 2p^2$	$1_{D^e} \quad 2s^2 2p 3s \quad 3_{P^o}$	5	3	6.01E-04	6.81E+08	-	-		
$2s^2 2p^2$	$1_{D^e} \quad 2s^2 2p 3s \quad 3_{P^o}$	5	5	7.72E-05	5.27E+07	-	-		
$2s^2 2p^2$	$1_{D^e} \quad 2s^2 2p 3s \quad 1_{P^o}$	5	3	5.48E-02	6.36E+10	5.30E-02	6.13E+10		
$2s^2 2p^2$	$1_{D^e} \quad 2s^2 2p 3d \quad 3_{F^o}$	5	5	7.88E-02	6.83E+10	6.81E-02	5.88E+10		
$2s^2 2p^2$	$1_{D^e} \quad 2s^2 2p 3d \quad 3_{F^o}$	5	7	1.03E-03	6.43E+08	-	-		
$2s^2 2p^2$	$1_{D^e} \quad 2s^2 2p 3d \quad 1_{D^o}$	5	5	1.15E-01	9.98E+10	1.23E-01	1.07E+11		
$2s^2 2p^2$	$1_{D^e} \quad 2s^2 2p 3d \quad 3_{D^o}$	5	3	6.47E-05	9.58E+07	-	-		
$2s^2 2p^2$	$1_{D^e} \quad 2s^2 2p 3d \quad 3_{D^o}$	5	5	3.24E-04	2.88E+08	-	-		
$2s^2 2p^2$	$1_{D^e} \quad 2s^2 2p 3d \quad 3_{D^o}$	5	7	5.04E-05	3.21E+07	-	-		
$2s^2 2p^2$	$1_{D^e} \quad 2s^2 2p 3d \quad 3_{P^o}$	5	3	4.50E-05	6.73E+07	-	-		
$2s^2 2p^2$	$1_{D^e} \quad 2s^2 2p 3d \quad 3_{P^o}$	5	5	1.85E-03	1.66E+09	-	-		
$2s^2 2p^2$	$1_{D^e} \quad 2s^2 2p 3d \quad 1_{F^o}$	5	7	8.28E-01	5.45E+11	8.05E-01	5.26E+11		
$2s^2 2p^2$	$1_{D^e} \quad 2s^2 2p 3d \quad 1_{P^o}$	5	3	8.40E-03	1.29E+10	1.01E-02	1.55E+10		
$2s^2 2p^2$	$1_{S^e} \quad 2s 2p^3 \quad 3_{D^o}$	1	3	1.91E-05	9.19E+04	1.79E-05	8.70E+04		
$2s^2 2p^2$	$1_{S^e} \quad 2s 2p^3 \quad 3_{P^o}$	1	3	6.24E-05	5.01E+05	5.94E-05	4.75E+05		
$2s^2 2p^2$	$1_{S^e} \quad 2s 2p^3 \quad 3_{S^o}$	1	3	9.66E-05	1.67E+06	8.22E-05	1.40E+06		
$2s^2 2p^2$	$1_{S^e} \quad 2s 2p^3 \quad 1_{P^o}$	1	3	2.05E-01	4.52E+09	2.03E-01	4.39E+09		
$2s^2 2p^2$	$1_{S^e} \quad 2s^2 2p 3s \quad 3_{P^o}$	1	3	8.24E-04	1.70E+08	-	-		
$2s^2 2p^2$	$1_{S^e} \quad 2s^2 2p 3s \quad 1_{P^o}$	1	3	9.38E-02	1.99E+10	8.69E-02	1.84E+10		
$2s^2 2p^2$	$1_{S^e} \quad 2s^2 2p 3d \quad 3_{D^o}$	1	3	1.72E-03	4.70E+08	-	-		

TABLE III. (Continued).

Transition				Present				[DEK]	
Initial Level	Final Level	g_i	g_k	f_l	A_l	f_l	A_l		
$2s^22p^2$	1_{Se} $2s^22p3d$	3_{Po}	1	3	6.78E-04	1.87E+08	-	-	
$2s^22p^2$	1_{Se} $2s^22p3d$	1_{Po}	1	3	1.15E+00	3.27E+11	1.12E+00	3.16E+11	

[DEK] Kelleher and Podobedova [9].

In Figure 2, we have compared the length values of transition probabilities from the two calculations. As seen from the figure, the agreement between the present and the other theoretical transition probabilities is very good with the exception for the $2s^22p^2$ $^3P_2^e \Rightarrow 2s2p^3$ $^3D_1^o$ transition. The average ratio between the two sets of data is $(A_l(\text{Present})/A_l(\text{DEK})) = 1.02$; thus, it shows that our calculated transition probabilities can be expected to be reliable to within 10 % for most of the transitions.

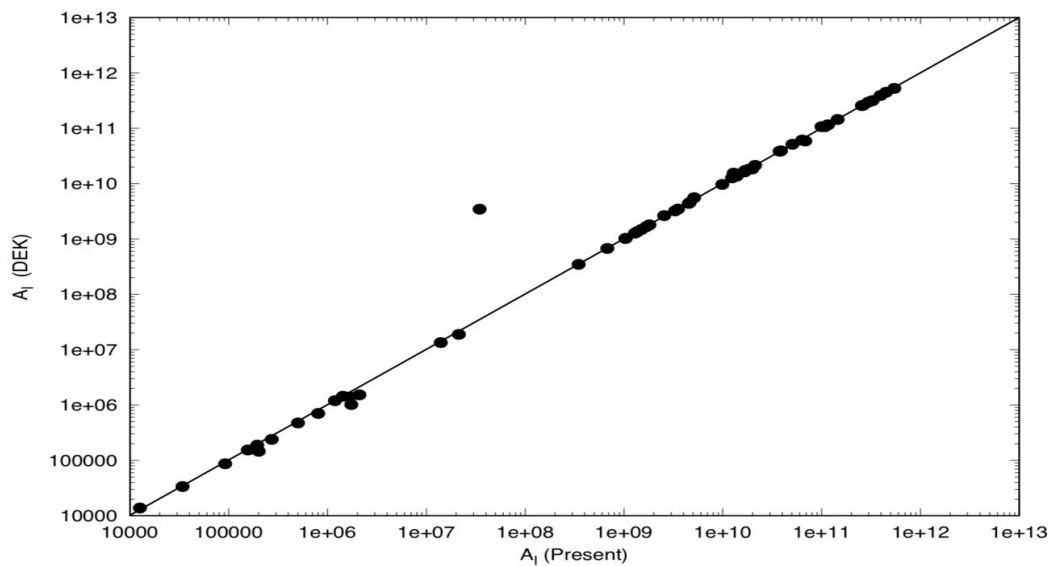


FIG. 2. Comparison between the calculated transition probabilities obtained in the present work (A_l) and the theoretical values (A_l) reported by Kelleher and Podobedova [9].

In Table IV, we have compared the present results for some E1 transitions among the terms of ground state $(1s^2)2s^22p^2$ and the excited states $2s2p^3$, $2s^22p3s$ and $2s^22p3d$ with Froese Fischer and Tachiev [5]. A very good agreement was obtained between the two calculations.

TABLE IV. Comparison of present of length and velocity oscillator strengths for some E1 transitions in Mg VII with CFF results.

Transition		Present				[CFF]		
Initial Level	Final Level	g_i	g_k	f_l	f_v	f_l	f_v	
$2s^22p^2$	$3p_e$ $2s2p^3$	$5S_o$	3	5	2.35E-06	4.45E-06	2.71E-06	3.57E-06
$2s^22p^2$	$3p_e$ $2s2p^3$	$5S_o$	5	5	3.93E-06	7.58E-06	4.11E-06	5.39E-06
$2s^22p^2$	$3p_e$ $2s2p^3$	$3D_o$	1	3	8.50E-02	8.74E-02	8.64E-02	8.35E-02
$2s^22p^2$	$3p_e$ $2s2p^3$	$3D_o$	3	3	1.87E-02	1.91E-02	1.90E-02	1.83E-02
$2s^22p^2$	$3p_e$ $2s2p^3$	$3D_o$	3	5	6.32E-02	6.52E-02	6.42E-02	6.22E-02
$2s^22p^2$	$3p_e$ $2s2p^3$	$3D_o$	5	3	5.81E-04	5.89E-04	5.90E-04	5.67E-04
$2s^22p^2$	$3p_e$ $2s2p^3$	$3D_o$	5	5	9.78E-03	9.97E-03	9.91E-03	9.56E-03
$2s^22p^2$	$3p_e$ $2s2p^3$	$3D_o$	5	7	6.60E-02	6.82E-02	6.70E-02	6.50E-02
$2s^22p^2$	$3p_e$ $2s2p^3$	$3p_o$	1	3	8.77E-02	9.30E-02	8.84E-02	8.64E-02
$2s^22p^2$	$3p_e$ $2s2p^3$	$3p_o$	3	1	3.03E-02	3.20E-02	3.06E-02	2.99E-02
$2s^22p^2$	$3p_e$ $2s2p^3$	$3p_o$	3	3	2.53E-02	2.68E-02	2.56E-02	2.50E-02
$2s^22p^2$	$3p_e$ $2s2p^3$	$3p_o$	3	5	3.37E-02	3.58E-02	3.39E-02	3.31E-02
$2s^22p^2$	$3p_e$ $2s2p^3$	$3p_o$	5	3	2.17E-02	2.29E-02	2.19E-02	2.14E-02

TABLE IV. (Continued).

Transition				Present				[CFF]	
Initial Level	Final Level	g_i	g_k	f_l	f_v	f_l	f_v		
$2s^22p^2$	$3p_e$	$2s2p^3$	$3p_o$	5	5	7.02E-02	7.43E-02	7.09E-02	6.91E-02
$2s^22p^2$	$3p_e$	$2s2p^3$	$1D_o$	3	5	1.58E-05	1.47E-05	1.49E-05	4.12E-05
$2s^22p^2$	$3p_e$	$2s2p^3$	$1D_o$	5	5	1.67E-04	1.69E-04	1.82E-04	1.72E-04
$2s^22p^2$	$3p_e$	$2s2p^3$	$3S_o$	1	3	1.10E-01	1.18E-01	1.10E-01	1.07E-01
$2s^22p^2$	$3p_e$	$2s2p^3$	$3S_o$	3	3	1.11E-01	1.19E-01	1.11E-01	1.08E-01
$2s^22p^2$	$3p_e$	$2s2p^3$	$3S_o$	5	3	1.14E-01	1.21E-01	1.13E-01	1.11E-01
$2s^22p^2$	$3p_e$	$2s2p^3$	$1p_o$	1	3	5.60E-06	8.20E-06	4.94E-06	5.61E-06
$2s^22p^2$	$3p_e$	$2s2p^3$	$1p_o$	3	3	1.99E-04	2.09E-04	2.05E-04	2.01E-04
$2s^22p^2$	$3p_e$	$2s2p^3$	$1p_o$	5	3	9.85E-06	9.14E-06	7.97E-06	7.28E-06
$2s^22p^2$	$3p_e$	$2s^22p3s$	$3p_o$	1	3	6.82E-02	6.84E-02	7.04E-02	6.88E-02
$2s^22p^2$	$3p_e$	$2s^22p3s$	$3p_o$	3	1	2.30E-02	2.30E-02	2.36E-02	2.31E-02
$2s^22p^2$	$3p_e$	$2s^22p3s$	$3p_o$	3	3	1.69E-02	1.69E-02	1.75E-02	1.71E-02
$2s^22p^2$	$3p_e$	$2s^22p3s$	$3p_o$	3	5	2.87E-02	2.88E-02	2.98E-02	2.90E-02
$2s^22p^2$	$3p_e$	$2s^22p3s$	$3p_o$	5	3	1.73E-02	1.74E-02	1.78E-02	1.74E-02
$2s^22p^2$	$3p_e$	$2s^22p3s$	$3p_o$	5	5	5.17E-02	5.18E-02	5.36E-02	5.24E-02
$2s^22p^2$	$3p_e$	$2s^22p3s$	$1p_o$	1	3	5.10E-04	5.18E-04	5.40E-04	5.26E-04
$2s^22p^2$	$3p_e$	$2s^22p3s$	$1p_o$	3	3	2.51E-04	2.53E-04	2.73E-04	2.60E-04
$2s^22p^2$	$3p_e$	$2s^22p3s$	$1p_o$	5	3	6.54E-05	6.81E-05	6.25E-05	6.06E-05

TABLE IV. (Continued).

Transition				Present				[CFF]	
Initial Level	Final Level	g_i	g_k	f_l	f_v	f_l	f_v		
$2s^2 2p^2$	$3p_e$ $2s^2 2p 3d$	$3F_o$	3	5	5.66E-05	5.61E-05	1.43E-04	1.45E-04	
$2s^2 2p^2$	$3p_e$ $2s^2 2p 3d$	$3F_o$	5	5	1.25E-03	1.24E-03	1.24E-03	1.25E-03	
$2s^2 2p^2$	$3p_e$ $2s^2 2p 3d$	$3F_o$	5	7	4.37E-03	4.33E-03	4.61E-03	4.67E-03	
$2s^2 2p^2$	$3p_e$ $2s^2 2p 3d$	$1D_o$	3	5	5.70E-03	5.65E-03	6.01E-03	6.07E-03	
$2s^2 2p^2$	$3p_e$ $2s^2 2p 3d$	$1D_o$	5	5	1.73E-04	1.74E-04	2.13E-04	2.12E-04	
$2s^2 2p^2$	$3p_e$ $2s^2 2p 3d$	$3D_o$	1	3	9.39E-01	9.32E-01	9.21E-01	9.14E-01	
$2s^2 2p^2$	$3p_e$ $2s^2 2p 3d$	$3D_o$	3	3	1.52E-01	1.51E-01	1.52E-01	1.51E-01	
$2s^2 2p^2$	$3p_e$ $2s^2 2p 3d$	$3D_o$	3	5	6.90E-01	6.85E-01	6.78E-01	6.73E-01	
$2s^2 2p^2$	$3p_e$ $2s^2 2p 3d$	$3D_o$	5	3	1.61E-03	1.59E-03	1.80E-03	1.78E-03	
$2s^2 2p^2$	$3p_e$ $2s^2 2p 3d$	$3D_o$	5	5	4.09E-02	4.05E-02	4.42E-02	4.38E-02	
$2s^2 2p^2$	$3p_e$ $2s^2 2p 3d$	$3D_o$	5	7	6.61E-01	6.56E-01	6.53E-01	6.48E-01	
$2s^2 2p^2$	$3p_e$ $2s^2 2p 3d$	$3p_o$	1	3	1.17E-01	1.17E-01	1.21E-01	1.20E-01	
$2s^2 2p^2$	$3p_e$ $2s^2 2p 3d$	$3p_o$	3	1	8.85E-02	8.82E-02	8.75E-02	8.67E-02	
$2s^2 2p^2$	$3p_e$ $2s^2 2p 3d$	$3p_o$	3	3	1.13E-01	1.12E-01	1.09E-01	1.08E-01	
$2s^2 2p^2$	$3p_e$ $2s^2 2p 3d$	$3p_o$	3	5	8.91E-03	8.95E-03	1.13E-02	1.14E-02	
$2s^2 2p^2$	$3p_e$ $2s^2 2p 3d$	$3p_o$	5	3	7.25E-02	7.23E-02	7.15E-02	7.09E-02	
$2s^2 2p^2$	$3p_e$ $2s^2 2p 3d$	$3p_o$	5	5	2.75E-01	2.74E-01	2.68E-01	2.66E-01	
$2s^2 2p^2$	$3p_e$ $2s^2 2p 3d$	$1F_o$	5	7	4.40E-06	4.84E-06	2.27E-05	2.21E-05	

TABLE IV. (Continued).

Transition		Present				[CFF]		
Initial Level	Final Level	g_i	g_k	f_l	f_v	f_l	f_v	
$2s^22p^2$	$3p_e$ $2s^22p3d$	$1p_o$	1	3	1.77E-03	1.77E-03	2.21E-03	2.18E-03
$2s^22p^2$	$3p_e$ $2s^22p3d$	$1p_o$	3	3	2.46E-04	2.43E-04	2.44E-04	2.32E-04
$2s^22p^2$	$3p_e$ $2s^22p3d$	$1p_o$	5	3	1.49E-05	1.43E-05	1.37E-05	1.36E-05
$2s^22p^2$	$1D_e$ $2s2p^3$	$5S_o$	5	5	1.96E-09	5.07E-09	2.04E-09	3.54E-09
$2s^22p^2$	$1D_e$ $2s2p^3$	$3D_o$	5	3	3.79E-06	7.21E-06	3.90E-06	4.66E-06
$2s^22p^2$	$1D_e$ $2s2p^3$	$3D_o$	5	5	1.10E-05	1.31E-05	1.11E-05	1.08E-05
$2s^22p^2$	$1D_e$ $2s2p^3$	$3D_o$	5	7	6.74E-05	7.85E-05	7.73E-05	1.19E-04
$2s^22p^2$	$1D_e$ $2s2p^3$	$3p_o$	5	3	2.33E-05	2.62E-05	2.62E-05	2.35E-05
$2s^22p^2$	$1D_e$ $2s2p^3$	$3p_o$	5	5	5.27E-06	4.23E-06	6.59E-06	6.54E-06
$2s^22p^2$	$1D_e$ $2s2p^3$	$1D_o$	5	5	2.07E-01	2.20E-01	2.08E-01	2.02E-01
$2s^22p^2$	$1D_e$ $2s2p^3$	$3S_o$	5	3	1.80E-05	2.03E-05	1.64E-05	1.63E-05
$2s^22p^2$	$1D_e$ $2s^22p3s$	$3p_o$	5	3	6.01E-04	5.67E-04	5.47E-04	5.54E-04
$2s^22p^2$	$1D_e$ $2s^22p3s$	$3p_o$	5	5	7.72E-05	7.60E-05	8.04E-05	8.24E-05
$2s^22p^2$	$1D_e$ $2s^22p3s$	$1p_o$	5	3	5.48E-02	5.24E-02	5.41E-02	5.37E-02
$2s^22p^2$	$1D_e$ $2s^22p3d$	$3F_o$	5	5	7.88E-02	7.79E-02	6.82E-02	6.86E-02
$2s^22p^2$	$1D_e$ $2s^22p3d$	$3F_o$	5	7	1.03E-03	1.01E-03	5.25E-03	5.48E-03
$2s^22p^2$	$1D_e$ $2s^22p3d$	$1D_o$	5	5	1.15E-01	1.13E-01	1.23E-01	1.24E-01
$2s^22p^2$	$1D_e$ $2s^22p3d$	$3D_o$	5	3	6.47E-05	6.56E-05	6.68E-05	6.65E-05

TABLE IV. (Continued).

Transition				Present				[CFF]	
Initial Level	Final Level	g_i	g_k	f_l	f_v	f_l	f_v		
$2s^22p^2$	1_{D^e} $2s^22p3d$	3_{D^o}	5	5	3.24E-04	3.22E-04	3.56E-04	3.47E-04	
$2s^22p^2$	1_{D^e} $2s^22p3d$	3_{D^o}	5	7	5.04E-05	4.86E-05	6.78E-05	7.08E-05	
$2s^22p^2$	1_{D^e} $2s^22p3d$	3_{P^o}	5	3	4.50E-05	4.44E-05	4.29E-05	2.27E-04	
$2s^22p^2$	1_{D^e} $2s^22p3d$	3_{P^o}	5	5	1.85E-03	1.83E-03	1.93E-03	1.93E-03	
$2s^22p^2$	1_{D^e} $2s^22p3d$	1_{F^o}	5	7	8.28E-01	8.15E-01	7.79E-01	7.78E-01	
$2s^22p^2$	1_{D^e} $2s2p^3$	1_{P^o}	5	3	8.40E-03	8.52E-03	8.01E-03	7.58E-03	
$2s^22p^2$	1_{S^e} $2s2p^3$	3_{D^o}	1	3	1.91E-05	1.97E-05	2.11E-05	2.06E-05	
$2s^22p^2$	1_{S^e} $2s2p^3$	3_{P^o}	1	3	6.24E-05	8.35E-05	6.69E-05	7.67E-05	
$2s^22p^2$	1_{S^e} $2s2p^3$	3_{S^o}	1	3	9.66E-05	9.71E-05	9.87E-05	9.44E-05	
$2s^22p^2$	1_{S^e} $2s2p^3$	1_{P^o}	1	3	2.05E-01	2.13E-01	2.06E-01	1.99E-01	
$2s^22p^2$	1_{S^e} $2s^22p3s$	3_{P^o}	1	3	8.24E-04	7.89E-04	7.34E-04	7.49E-04	
$2s^22p^2$	1_{S^e} $2s^22p3s$	1_{P^o}	1	3	9.38E-02	9.02E-02	8.82E-02	8.90E-02	
$2s^22p^2$	1_{S^e} $2s^22p3d$	3_{D^o}	1	3	1.72E-03	1.69E-03	1.71E-03	1.74E-03	
$2s^22p^2$	1_{S^e} $2s^22p3d$	3_{P^o}	1	3	6.78E-04	6.69E-04	7.83E-04	8.01E-04	
$2s^22p^2$	1_{S^e} $2s^22p3d$	1_{P^o}	1	3	1.15E+00	1.13E+00	1.06E+00	1.07E+00	

[CFF] Froese Fischer and Tachiev [5].

The ratios of the present oscillator strengths in length and velocity formulations have been plotted in Figure 3. As seen from the figure, we have a very good agreement between the two formulations. The good point distribution along the straight line is obtained for the stronger lines. The average ratio among the two sets of data is $(f_l/f_v) = 0.96$, accordingly this means that our calculations can be expected to be reliable to within 10% for most transitions. The present length oscillator strengths have been compared with the results of Froese Fischer and Tachiev [5] in Figure 4. The agreement between the two MCHF calculations is very good for all transitions, with the exceptions of the $2s^22p^2\ ^3P_2^e \Rightarrow 2s^22p3d\ ^1F_3^o$, $2s^22p^2\ ^3P_1^e \Rightarrow 2s^22p3d\ ^3F_2^o$ and $2s^22p^2\ ^1D_2^e \Rightarrow 2s^22p3d\ ^3F_3^o$ transitions. The average ratio among the two sets of data is $(f_l(\text{Present})/f_l(\text{CFF})) = 0.96$, hence; again indicating an accuracy of 10% for most of the transitions.

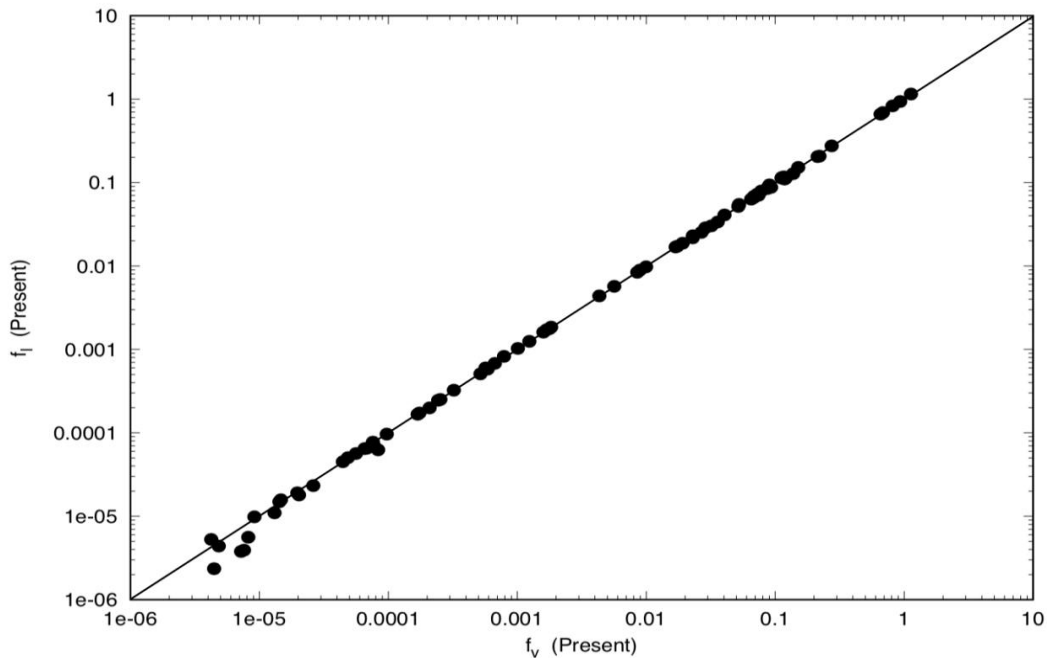


FIG. 3. Comparison between length and velocity of the present oscillator strengths for some E1 transitions.

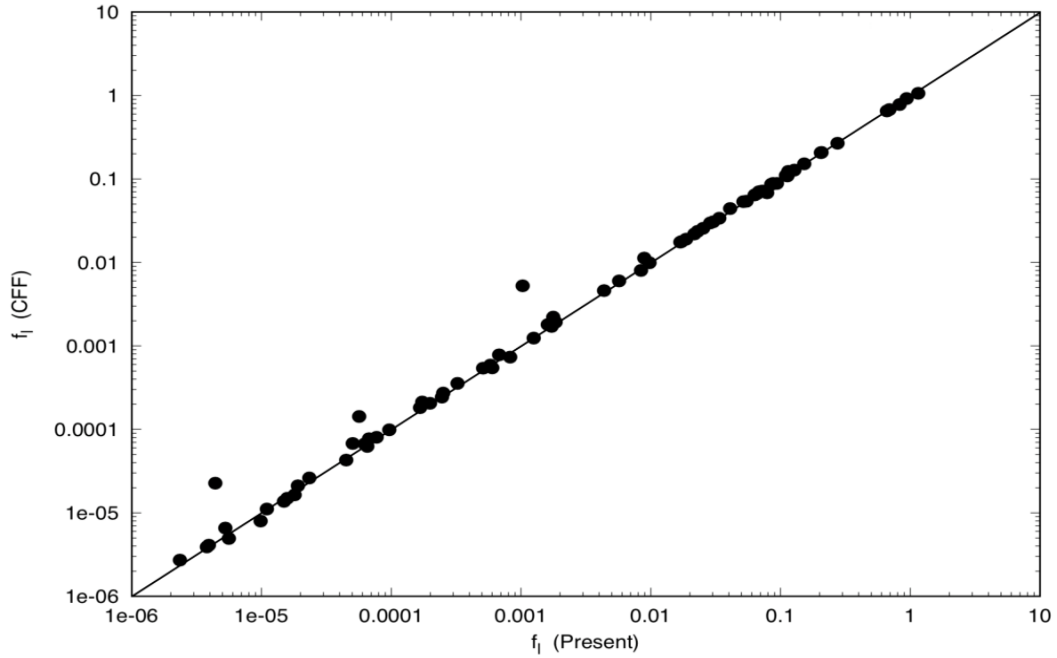


FIG. 4. Comparison between length forms of the present and CFF [5] oscillator strengths for some E1 transitions.

In Figure 5, we have represented the ratio of the present velocity and length of the oscillator strengths as a function of the present length oscillator strengths. The two lines in this figure display a deviation. As seen from the figure that the agreement between the present velocity and length of the oscillator strength values is within 20 % for most of the transitions.

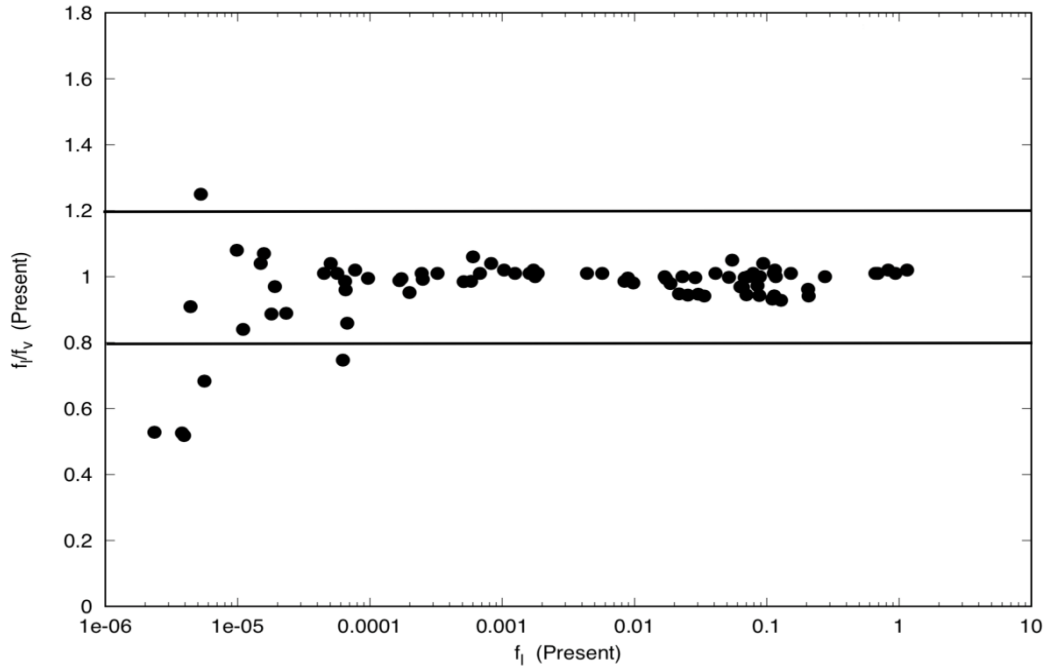


FIG. 5. The ratio between length and velocity forms of the present oscillator strengths as a function of length form of present oscillator strengths for some E1 transitions has been shown.

3.3.2 Transition Probabilities for (E2 and M1) Forbidden Transitions

In this part, we have calculated transition probabilities for forbidden E2 and M1 transitions and presented in Table V. The present values have been compared with Kelleher and Podobedova [9] and with Froese Fischer and Tachiev [13]. The agreement between the present values and the two calculations is excellent, with exception for one transition $2s^2 2p^2 \ ^3P_1^e \Rightarrow 2p^4 \ ^1S_0^e$.

TABLE V. Comparison of present transition probabilities (s^{-1}) for the forbidden transitions in Mg VII with CFF and DEK results.

Transition						Present	[CFF]	[DEK]
Initial Level	Final Level	g_i	g_k	Type	A_I	A_I	A_I	
$2s^2 2p^2 \ 3p_e$	$2s^2 2p^2 \ 3p_e$	1	5	E2	2.17E-07	2.32E-07	2.24E07	
$2s^2 2p^2 \ 3p_e$	$2s^2 2p^2 \ 3p_e$	3	5	E2	4.45E-08	4.68E-08	4.54E-08	
$2s^2 2p^2 \ 3p_e$	$2s^2 2p^2 \ 3p_e$	1	3	M1	2.41E-02	2.54E-02	2.43E-02	
$2s^2 2p^2 \ 3p_e$	$2s^2 2p^2 \ 3p_e$	3	5	M1	7.83E-02	8.03E-02	7.95E-02	
$2s^2 2p^2 \ 3p_e$	$2s^2 2p^2 \ 1D_e$	1	5	E2	1.29E-04	1.27E-04	1.25E-04	
$2s^2 2p^2 \ 3p_e$	$2s^2 2p^2 \ 1D_e$	3	5	E2	3.68E-04	3.53E-04	3.34E-04	
$2s^2 2p^2 \ 3p_e$	$2s^2 2p^2 \ 1D_e$	5	5	E2	2.05E-03	1.96E-03	1.93E-03	
$2s^2 2p^2 \ 3p_e$	$2s^2 2p^2 \ 1D_e$	3	5	M1	1.24E+00	1.23E+00	1.20E+00	
$2s^2 2p^2 \ 3p_e$	$2s^2 2p^2 \ 1D_e$	5	5	M1	3.25E+00	3.22E+00	3.13E+00	
$2s^2 2p^2 \ 3p_e$	$2s^2 2p^2 \ 1S_e$	5	1	E2	3.89E-02	3.88E-02	3.85E-02	
$2s^2 2p^2 \ 3p_e$	$2s^2 2p^2 \ 1S_e$	3	1	M1	3.72E+01	3.71E+01	3.62E+01	
$2s^2 2p^2 \ 1D_e$	$2s^2 2p^2 \ 1S_e$	5	1	E2	4.24E+00	3.89E+00	3.95E+00	
$2p^4 \ 3p_e$	$2p^4 \ 3p_e$	5	3	E2	1.47E-07	-	-	
$2p^4 \ 3p_e$	$2p^4 \ 3p_e$	5	1	E2	1.13E-06	-	-	
$2p^4 \ 3p_e$	$2p^4 \ 3p_e$	3	1	M1	3.36E-02	-	-	
$2p^4 \ 3p_e$	$2p^4 \ 3p_e$	5	3	M1	1.91E-01	-	-	
$2p^4 \ 3p_e$	$2p^4 \ 1D_e$	1	5	E2	3.43E-06	-	-	

TABLE V. (Continued).

Transition						Present	[CFF]	[DEK]	
Initial Level	Final Level	g_i	g_k	Type	A_l	A_l	A_l		
2p ⁴	3p _e	2p ⁴	1D _e	5	5	E2	1.20E-03	-	-
2p ⁴	3p _e	2p ⁴	1D _e	3	5	E2	1.36E-04	-	-
2p ⁴	3p _e	2p ⁴	1D _e	3	5	M1	6.67E-01	-	-
2p ⁴	3p _e	2p ⁴	1S _e	5	1	E2	4.26E-01	-	-
2p ⁴	3p _e	2p ⁴	1S _e	3	1	M1	4.73E+01	-	-
2p ⁴	1D _e	2p ⁴	1S _e	5	1	E2	1.00E+02	-	-
2s ² 2p ²	3p _e	2p ⁴	3p _e	1	5	E2	6.94E+03	-	7.34E+03
2s ² 2p ²	3p _e	2p ⁴	3p _e	5	1	E2	3.47E+04	-	3.67E+04
2s ² 2p ²	3p _e	2p ⁴	3p _e	3	5	E2	1.54E+04	-	1.64E+04
2s ² 2p ²	3p _e	2p ⁴	3p _e	5	3	E2	2.59E+04	-	2.73E+04
2s ² 2p ²	3p _e	2p ⁴	3p _e	3	3	E2	8.74E+03	-	-
2s ² 2p ²	3p _e	2p ⁴	3p _e	5	5	E2	1.19E+04	-	-
2s ² 2p ²	3p _e	2p ⁴	3p _e	1	3	M1	4.63E-01	-	4.15E-01
2s ² 2p ²	3p _e	2p ⁴	3p _e	3	1	M1	1.61E+00	-	1.45E+00
2s ² 2p ²	3p _e	2p ⁴	3p _e	3	3	M1	4.83E-11	-	-
2s ² 2p ²	3p _e	2p ⁴	3p _e	3	5	M1	1.56E+00	-	1.43E+00
2s ² 2p ²	3p _e	2p ⁴	3p _e	5	3	M1	2.34E+00	-	2.13E+00
2s ² 2p ²	3p _e	2p ⁴	3p _e	5	5	M1	1.26E-02	-	-

TABLE V. (Continued).

Transition							Present	[CFF]	[DEK]
Initial Level	Final Level	g_i	g_k	Type	A_I	A_I	A_I		
$2s^22p^2$	$3p_e$ $2p^4$	$1D^e$	1	5	E2	3.73E-01	-	6.89E-01	
$2s^22p^2$	$3p_e$ $2p^4$	$1D^e$	3	5	E2	2.71E+01	-	3.27E+01	
$2s^22p^2$	$3p_e$ $2p^4$	$1D^e$	5	5	M1	2.31E+00	-	-	
$2s^22p^2$	$3p_e$ $2p^4$	$1D^e$	3	5	M1	6.97E-01	-	6.46E-01	
$2s^22p^2$	$3p_e$ $2p^4$	$1D^e$	5	5	E2	1.94E+01	-	-	
$2s^22p^2$	$3p_e$ $2p^4$	$1S^e$	5	1	E2	1.27E+01	-	1.83E+01	
$2s^22p^2$	$3p_e$ $2p^4$	$1S^e$	3	1	M1	4.04E+00	-	3.42E-01	
$2s^22p^2$	$1S^e$ $2p^4$	$3p_e$	1	5	E2	2.75E-02	-	4.12E-02	
$2s^22p^2$	$1S^e$ $2p^4$	$3p_e$	1	3	M1	5.98E-01	-	5.73E-01	
$2s^22p^2$	$1S^e$ $2p^4$	$1D^e$	1	5	E2	4.02E+03	-	-	
$2s^22p^2$	$1D^e$ $2p^4$	$3p_e$	5	1	E2	4.95E+00	-	4.81E+00	
$2s^22p^2$	$1D^e$ $2p^4$	$3p_e$	5	3	E2	2.66E+01	-	2.98E+01	
$2s^22p^2$	$1D^e$ $2p^4$	$1D^e$	5	5	E2	4.53E+04	-	-	
$2s^22p^2$	$1D^e$ $2p^4$	$1S^e$	5	1	E2	5.83E+04	-	6.36E+04	

[CFF] Froese Fischer and Tachiev [13].

[DEK] Kelleher and Podobedova [9].

CHAPTER 4

CONCLUSION

We have presented our calculations of energy levels, lifetimes, and oscillator strengths for the dipole allowed transitions and forbidden transitions of Mg VII arising from the $(1s^2)2s^22p^2$, $2s2p^3$, $2p^4$, $2s^22p3s$, $2s^22p3p$, $2s2p^2(^4P)3s$ and $2s^22p3d$ configurations. The present energy results have been compared with the results from the NIST compilation [10], the SS program calculation by Bhatia and Doschek [11], the CIV3 code calculation by Aggarwal [12], MCHF calculation by Froese Fischer and Tachiev [13], and the GRASP program calculation by Zhang and Sampson [14]. The present lifetimes results have been compared with Lestinsky et al. [8] and Froese Fischer and Tachiev [13]. The present results of oscillator strengths and transition probabilities compared with Kelleher and Podobedova [9] and Froese Fischer and Tachiev [5,13].

Comparisons between energy levels calculated by the different atomic methods indicate that the agreement with NIST results is satisfactory, with the exception of few energy levels. Unfortunately, several energy levels are not listed in the NIST atomic database. The comparative studies of atomic structure data validate our results.

Transition probabilities and oscillator strengths for transitions between the $(1s^2)2s^22p^2$, $2s2p^3$, $2p^4$, $2s^22p3s$, and $2s^22p3d$ configurations have been computed by many scientists. We have compared our results for both allowed (E1) and forbidden (M1

and E2) types of transitions. The comparison between the present values and the available other two calculations displays very good agreement for most of the transitions. The differences between the present results and other calculations are of the order of 10% or better for strong transitions.

REFERENCES

1. Y. Kojima, *Materials Transactions*, **42**, 1154 (2001).
2. J. E. McMurry and R. C. Fay, *Chemistry*, 6th Ed. (Prentice Hall, 2012).
3. J. R. de Laeter, J. K. Böhlke, P. De bièvre, H. Hidaka, H. S. Peiser, K. J. R. Rosman, and P. D. P. Taylor, *Pure Appl. Chem.*, **75**, 683 (2003).
4. J. Meija et al, *Pure Appl. Chem.*, **88**, 265 (2016).
5. G. Tachiev and C. Froese Fischer, *Can. J. Phys.*, **79**, 955 (2001). Original Data Available Online by (https://nlte.nist.gov/MCHF/Elements/Mg/C_12.4.html).
6. K. M. Aggarwal, *The Astrophys. J. (Supplement Series)*, **56**, 303 (1984).
7. S. S. Tayal and A. M. Sossah, *A&A*, **574**, A87 (2015).
8. M. Lestinsky, N. R. Badnell, D. Bernhardt, D. Bing, M. Grieser, M. Hahn, J. Hoffmann, B. Jordon-Thaden, C. Krantz, O. Novotny', D. A. Orlov, R. Repnow, A. Shornikov, A. Müller, S. Schippers, A. Wolf, and D. W. Savin, *The Astrophys. J.* **758**, 1 (2012).
9. D. E. Kelleher and L. I. Podobedova, *J. Phys. Chem. Ref. Data*, **37**, 267 (2008).
10. A. Kramida, Yu. Ralchenko, and J. Reader, and NIST ASD Team (2018). *NIST Atomic Spectra Database*, 5.3, [Online]. Available: <http://physics.nist.gov/asd>. National Institute of Standards and Technology, Gaithersburg, MD.
11. A. K. Bhatia and G. A. Doschek, *At. Data Nucl. Data Tables*, **60**, 145 (1995).

12. K. M. Aggarwal, *The Astrophys. J. (Supplement Series)*, **118**, 589 (1998).
13. C. Froese Fischer and G. Tachiev, *At. Data Nucl. Data Tables*, **87**, 1 (2004).
14. H. L. Zhang and D. H. Sampson, *At. Data Nucl. Data Tables*, **63**, 275 (1996) *At. Data Nucl. Data Tables*, **65**, 183 (1997).
15. B. H. Bransden and C.J. Joachain, *Physics of Atoms and Molecules*, (Longman Scientific and Technical, 1983).
16. C. Froese Fischer, T. Brage, and P. Jönsson, *Computational Atomic Structure: An MCHF Approach*, Scanned by Terminator, (Institute of Physics Publishing, Bristol and Philadelphia, 1997).
17. J. Griffiths, *Introduction to Quantum Mechanics*, (Prentice Hall, Inc., 1995).